

To the Graduate Council:

I am submitting herewith a thesis written by Kelly Plummer entitled "Contact Metamorphism of Calc-Silicate Rocks in the Belmont Contact Aureole, Central Nevada." I have examined the final electronic copy of this thesis for form and content and recommend that it be accepted in partial fulfillment of the requirements for the degree of Master of Science with a major in Geology.

Theodore Labotka

Major Professor

We have read this thesis
and recommend its acceptance:

Claudia Mora

Kula Misra

Accepted for the Council:

Anne Mayhew

Vice Chancellor and
Dean of Graduate Studies

(original signatures on file with official student records)

Contact Metamorphism of Calc-Silicate Rocks in the Belmont Contact Aureole, Central Nevada

A Thesis
Presented for the
Master of Science
Degree
The University of Tennessee, Knoxville

Kelly Plummer
May 2006

ABSTRACT

This study focuses on the contact metamorphism of the Ordovician Zanzibar and Toquima Formations by the Cretaceous Belmont Pluton in central Nevada. I mapped the distributions of tremolite and diopside to determine the location of isograds. These isograds are the result of the reactions: $8 \text{ quartz} + 5 \text{ dolomite} + \text{H}_2\text{O} = 3 \text{ calcite} + \text{tremolite} + 7 \text{ CO}_2$ and $\text{tremolite} + 2 \text{ quartz} + 3 \text{ calcite} = 5 \text{ diopside} + 3 \text{ CO}_2 + \text{H}_2\text{O}$. Pressure of metamorphism is estimated at between 4 kbar and 1 kbar, but is not definite because of uncertainty in the amount of overburden at the time of metamorphism. Temperatures of metamorphism ranged from 400 to 560 °C for the tremolite isograd and 450 to 565 °C for the diopside isograd. Fluid compositions ranged from $X(\text{CO}_2) = 0.25$ to 0.98. Mass balance calculations show that change in volume decreased with increasing distance from the contact ($98.9 \text{ cm}^3/\text{kg}$ to $5.2 \text{ cm}^3/\text{kg}$) which corresponds to loss in CO_2 . Toquima carbon and oxygen isotope values increase with increasing distance from the pluton which is indicative of contact metamorphism. The $\delta^{18}\text{O}$ (SMOW) values for both calcite and dolomite in Zanzibar samples show no pattern of decrease with increasing metamorphic grade. Calcite values close to the pluton range from 15.7‰ to 21.2‰ and lower grade samples range from 15.0‰ to 18.6‰. The $\delta^{13}\text{C}$ (PDB) values are lower (-8.9‰ to -5.2‰) in higher grade samples. Low grade samples range from -6.6‰ to -0.8‰. Carbon isotopic values in Zanzibar samples do not increase with increasing distance from the pluton, but these values are systematic with the extent of reaction. There is no relationship between Zanzibar $\delta^{18}\text{O}$ values and

change in volume or change in CO₂. This shows there is no correlation between Zanzibar oxygen isotopic values and metamorphic reactions resulting from the emplacement of the pluton. The best explanation for the altered oxygen isotopic values is Tertiary volcanic activity. This activity is thought to be responsible for the formation of gold and silver ore deposits in the area of Belmont Nevada.

TABLE OF CONTENTS

Chapter	Page
I. INTRODUCTION	1
II. BACKGROUND	3
Description of Units.....	3
Tectonic Setting.....	4
Geologic Description of Field Area.....	6
III. ANALYTICAL TECHNIQUES	8
Petrography.....	8
Carbon and Oxygen Isotope Analysis.....	8
Bulk Chemical Analysis.....	9
IV. PETROGRAPHY OF MARBLES	10
Low Grade Marbles.....	10
Tremolite Zone Marbles.....	11
Diopside Zone Marbles.....	11
V. TEMPERATURE AND FLUID COMPOSITION	13
VI. MASS BALANCE	15
Mass Balance Calculations.....	15
Determining Changes in Volume and CO ₂	16
VII. BULK CHEMISTRY	18
VIII. STABLE ISOTOPES	19
Zanzibar Isotopic Data.....	19
Toquima Isotopic Data.....	20
Comparison of Zanzibar and Toquima Values.....	20
Comparison of Dolomite and Calcite Oxygen Isotopic Data.....	21
IX. DISCUSSION	22
Carbon Isotopes.....	22
Oxygen Isotopes.....	22
Oxygen Isotopes and Change in Volume.....	22
Alteration of Oxygen Isotopic Values.....	23
X. CONCLUSION	24
LIST OF REFERENCES	25
APPENDICES	28
VITA	60

LIST OF TABLES

Table		Page
B-1	Whole rock analysis	51
B-2	Mineral assemblages of Zanzibar and Toquima marbles	54
B-3	Metamorphic mass-balance	57
B-4	Calcite isotopic values	58
B-5	Dolomite isotopic values	59

LIST OF FIGURES

Figure	Page
A-1 Geologic map of Belmont Area by Shaw, 2000	29
A-2 Geologic map of field area	30
A-3 Foliated Marbles in the Zanzibar Formation	31
A-4 Field map of sample distributions and mineral isograds	32
A-5 Bulk composition of low grade, tremolite zone, and diopside zone assemblages projected on to the MgO-CaO-SiO ₂ diagram	33
A-6 T-X diagram for the CaO-MgO-SiO ₂ -H ₂ O-CO ₂ system at 4 kbar calculated using Thermocalc	34
A-7 T-X diagram for the CaO-MgO-SiO ₂ -H ₂ O-CO ₂ system at 1 kbar calculated using Thermocalc	35
A-8 T-X diagram for the CaO-MgO-SiO ₂ -H ₂ O-CO ₂ system at 2 kbar, after Hover-Granath et al, (1983)	36
A-9 Change in volume versus distance from the pluton	37
A-10 Bulk compositions of 8 limestone samples from the Zanzibar and Toquima formations determined by X-ray fluorescence	38
A-11 Distribution of calcite $\delta^{18}\text{O}$ values (SMOW)	39
A-12 Distribution of calcite $\delta^{13}\text{C}$ values (PDB)	40
A-13 Plot of $\delta^{18}\text{O}$ versus distance from the pluton	41
A-14 Plot of $\delta^{13}\text{C}$ versus distance from the pluton	42
A-15 Distribution of dolomite $\delta^{18}\text{O}$ values (SMOW)	43
A-16 Distribution of dolomite $\delta^{13}\text{C}$ values (PDB)	44
A-17 Plot of $\delta^{18}\text{O}$ and $\delta^{13}\text{C}$ calcite and dolomite values for Zanzibar and Toquima marbles	45
A-18 Plot of $\delta^{18}\text{O}$ calcite and dolomite values for Zanzibar and Toquima marbles	46
A-19 Plot of $\delta^{13}\text{C}$ and F(CO ₂) for nine Zanzibar samples	47
A-20 Plot of calcite $\delta^{18}\text{O}$ and change in volume values for Zanzibar marbles	48
A-21 Plot of $\delta^{18}\text{O}$ and F(CO ₂) for nine Zanzibar samples	49
A-22 CL image of a Zanzibar sample showing secondary calcite and luminescent grain boundaries	50

CHAPTER I INTRODUCTION

Calc-silicates make up a small part of the earth's crust but their metamorphism is significant because it can provide information about the metamorphic fluid phase as well as pressure and temperature conditions. The metamorphism of siliceous dolomites characteristically includes the sequence of minerals talc, tremolite, diopside, forsterite, wollastonite, periclase, monticellite, ackermanite, tilleyite, spurrite, rankinite, merwintite, and larnite. The metamorphism of calc-silicates differs from other rocks in that it involves both H₂O and CO₂ during progressive metamorphism.

Stable isotopes are a great tool for interpreting the history of contact metamorphism. Studies have defined the character of fluid flow, source, and flux in metamorphic terranes. Isotopic patterns have been used to help interpret many processes involving mass-transport such as diffusion, recrystallization, fluid infiltration, volatilization, metasomatism, and heat flow (Baumgartner and Valley, 2001). Oxygen and carbon isotopes are extremely useful since they reveal the origin and isotopic composition of fluids. They can also show the relative amounts of dehydration, decarbonation, and infiltration (Nabelek et al. 1984). In most cases, a coupled trend of isotope values and metamorphic mineral assemblage is observed. For example, rocks of higher metamorphic grade usually have lower $\delta^{18}\text{O}$ and $\delta^{13}\text{C}$ values.

Fluid infiltration may possibly change the bulk composition of a rock by mass transfer (Spear, 1993). Fluids can remove more soluble elements (Fe, K,

Ba, Rb, and Sr) and leave behind more insoluble elements (Al and Ti). Mass balance calculations can be used to determine the changes in mineral assemblage along with changes in the amounts of CO₂ and H₂O. This information can be used to determine the changes in solid volume and the creation of porosity (Labotka et al. 1984).

This study examined contact metamorphism of limestone intruded by the Cretaceous Belmont pluton in central Nevada (Figure A-1¹). It focused on a suite of samples collected from the Ordovician Zanzibar Formation, the Ordovician Toquima Formation and the Cretaceous Belmont Pluton. Zanzibar and Toquima samples can be traced across strike up to 0.8 km from the pluton (Figure A-2). The purpose of this study was to examine mineral assemblages, sequence of isograds, spacing of isograds, direction of metamorphic grade, oxygen isotopes, carbon isotopes, changes in volume, and the movement of volatiles (CO₂ and H₂O). These were used to develop a metamorphic history of the Zanzibar and Toquima Formations.

This location also presents some features that make it unusual compared to many other areas of contact metamorphism. First, the Zanzibar limestone was deformed prior to the intrusion of the Belmont pluton. Second, the Cretaceous Round Mountain pluton is in very close proximity to the contact between the Zanzibar and the Belmont pluton. Third, there are two Tertiary calderas in the area.

¹ All figures and tables are located in the Appendices

CHAPTER II BACKGROUND

Description of Units

Figure A-1 shows the locations of the Zanzibar Formation, Toquima Formation, and the Belmont Pluton in the area of Belmont, Nevada. The Ordovician Zanzibar Formation is an interlayered marine sedimentary sequence consisting of limestone and argillite. It is usually thin to medium bedded with some of the limestone being cherty. The Zanzibar is in contact with the eastern part of the Belmont pluton. These rocks have typically been metamorphosed into silicified argillite, schist, calc-silicate-mineralized limestone, dolostone, and jasperoid. The Zanzibar is Whiterockian in age (~472 – 460 Ma). Whiterockian age rocks from other localities in the Toquima Range exhibit an abundance of echinoderms and bryozoans fossils, which were not found in Zanzibar limestone at this location. The original thickness of the Zanzibar Formation is unknown because of extreme deformation caused by earlier tectonic activity (Shaw, 2003). Thrust plates underlying the Zanzibar include the Harkless Formation (Ordovician) and the Toquima Formation (Ordovician) and overlying thrust plates include a Cambrian siltstone unit, the Goldhill Formation (Cambrian) and the Mayflower Formation (Cambrian).

The Toquima formation is characteristically composed of thin bedded, interlayered, marine sedimentary rocks composed of argillite, limestone, siltstone, and quartzite. Many rocks have been metamorphosed to silicified argillite, schist, calc-silicate mineralized limestone, dolostone, and jasperoid. The unit is very

deformed by laminar flow, folding, and faulting. The original thickness of the unit can not be determined because of deformation. The age of the unit is Mohawkian (Middle Ordovician), based on the fossil record (Shaw, 2002).

The Belmont Pluton is an oval shaped granite pluton, ~11 x 19 km in size. The pluton is located just to the northwest of the town of Belmont, Nevada. The pluton grades upward from a coarse-grained granite to porphyritic, coarse-grained granite. The pluton intrudes older, deformed sedimentary Paleozoic rocks (Figure A-1). The age of the granite is 84.5 to 84.8 Ma by Rb-Sr whole rock isochrons (Shaw, 2002).

Tectonic Setting

The Cordilleran orogenic belt was largely created from predominately marine sedimentary rocks that deposited on the rifted western margin of Laurentia during Neoproterozoic-early Paleozoic time. These rocks became thicker and of deeper marine character westward from the Wasatch hinge line, which marks the estimated eastern edge of a region of considerable rifting in the Precambrian crystalline basement.

The Proterozoic succession ranges in thickness from ~4 km to >10 km and is composed mainly of siliclastic rocks with small quantities of carbonate rocks. The Paleozoic succession is composed of up to ~12 km of mostly carbonate rocks in western Utah and Nevada (Pluijm and Marsh, 1997).

The Paleozoic history of the Cordillera can be described as one of continued passive-margin sedimentation with little or no tectonic activity. There are several tectonic fragments of island arcs and backarc sequences, ranging in

age from Cambrian to Triassic, which can be seen in the western part of the Cordillera. During the Paleozoic, the North American shelf experienced times of regional subsidence and uplift with little deformation. The formation of the Roberts Mountain Thrust is an exception. It formed during the Antler Orogeny (~320 Ma), which caused earlier deposited sedimentary rock to be obducted during the closing of basins (DeCelles, 2004).

It was during the Antler Orogeny that the Zanzibar Formation along with other lower Paleozoic marine sedimentary rocks were thrust onto the continent. A result of this deformation was the creation of several thrust plates in the area of the Toquima Range in central Nevada. These thrust plates are composed of (in chronological order) the lower Mayflower Formation, Gold Hill Formation, Cambrian siltstone, Zanzibar Formation, Toquima Formation, Harkless Formation, and a Paleozoic limestone unit. These thrust plates were generally very deformed during emplacement with the lower plates being more severely deformed than the higher plates (Shaw, 2002).

In the Cretaceous, three granitic plutons intruded the deformed Paleozoic sedimentary rocks. These three plutons are the Round Mountain, Belmont, and the Pipe Springs pluton. The Round Mountain and Belmont plutons intruded and crystallized by ~80 Ma. The Pipe Springs formed at ~75 Ma (Shaw, 2002). The Round Mountain pluton may have contributed to the metamorphism of the Zanzibar because of its close proximity to the Belmont aureole (Figure A-1).

Two calderas formed in and around the Toquima Range during the Tertiary. These are the Mount Jefferson and Manhattan (Figure A-1). The Mount

Jefferson caldera formed at ~27 Ma and the Manhattan caldera formed at ~24.5 Ma (Shaw, 2002). The closing stages of igneous activity around the Jefferson caldera produced significant precious metal mineralization. This period saw the formation of several volcanic units in the area of the caldera along with the formation of the Round Mountain gold deposit, which formed at ~26.0 Ma. The Manhattan caldera formed with the eruption of the Round Rock formation, ~24.5 Ma. Eruptive megabreccias were emplaced during the formation of the caldera. Resurgent dacite and andesite magmas intruded the caldera before its collapse. Around the time the caldera was forming, several ash flow tuffs were deposited in the southern Toquima Range from an outside source. The Manhattan is also a location of gold and silver deposits. It is believed that these deposits were formed by a mineralization event that occurred at ~16 Ma. One possible explanation for the formation of these deposits is the emplacement of rhyolite necks at time of the mineralization event.

Geologic Description of Field Area

The field area of this project is shown in Figures A-1 and A-2. The field area consists of three geologic units, the Belmont pluton, the Zanzibar Formation, and the Toquima Formation. The Belmont pluton is composed of granite. The Zanzibar is composed mostly of metamorphosed limestone, argillites, and some jasperoid. Tremolite can also be seen as prismatic and fibrous crystals in the marbles particularly in the area of Hillen Canyon and the northern half of Snowbird Canyon (Figure A-3). Dark metamorphosed shale was found at the contact between the Zanzibar Formation and Belmont pluton, but no metamorphic

phases could be observed in hand sample. The Toquima Formation is very similar to the Zanzibar Formation, but contains quartzite. Both units are deformed, with foliated textures. The boundary between the Toquima Formation and Zanzibar Formation is marked by the appearance of quartzite and the presence of a thrust fault (Figure A-1 and A-2). The orientation of almost all measured strikes of foliation parallels the contact of the Zanzibar Formation and the Belmont pluton (Figure A-2). Most veins seemed to parallel foliation (Figure A-3). This indicates the majority of the deformation within the field area can be attributed to intrusion of the pluton.

CHAPTER III ANALYTICAL TECHNIQUES

Petrography

This project began with mapping the area shown in Figure A-1. This included the mapping of geologic units (Zanzibar Formation, Toquima Formation, and Belmont Pluton), geologic structures, and the collection of samples. All rock samples were examined in thin section to determine mineral assemblages. Some thin section and powdered samples were examined using the Siemens D500 X-ray diffractometer (XRD) at the University of Tennessee. The XRD was set at -40.0 KeV and -30.0 mA. The step size used for scanning was 0.02° and the count rate used was 0.02° per sec. Two samples were analyzed using cathodoluminescence. Polished thin sections were analyzed using a ELM-3RP SpectruMedix Luminoscope.

Carbon and Oxygen Isotope Analysis

Twenty-three samples from both the Zanzibar Formation and the Toquima Formation were analyzed for their oxygen and carbon isotopic compositions. Oxygen and carbon isotopic data for calcite and dolomite samples were collected using 3-5 mg of powdered carbonate samples reacted with 100% orthophosphoric acid. Samples containing only calcite were reacted at 120°C using the Finnigan MAT Carboflo acid bath connected to a Delta Plus multi-collector dual-inlet gas source mass spectrometer at the University of Tennessee. All data were corrected for 25°C . The other samples, containing both calcite and dolomite, were reacted

at 25°C in side arm vessels over a period of twenty-four hours, or until the calcite was completely dissolved. Samples containing dolomite were reacted at 25°C over a period of forty-eight hours, or until the entire sample was dissolved. The CO₂ released from these reactions was extracted and cryogenically cleaned in a high-vacuum extraction line by using cryogenic cleaning. The CO₂ was collected and analyzed on the dual-inlet gas source mass spectrometer. The calcite standards were ANU-M2 ($\delta^{13}\text{C}=2.81$ and $\delta^{18}\text{O}=23.32$) and CHCC ($\delta^{13}\text{C}=-10.66$ and $\delta^{18}\text{O}=21.08$) and the dolomite standard used was Brumado dolomite ($\delta^{13}\text{C}=-1.469$ and $\delta^{18}\text{O}=14.027$). The error for samples containing only calcite was ± 0.29 for oxygen and ± 0.07 for carbon.

Bulk Chemical Analysis

Twenty-two samples from the three metamorphic zones were analyzed for their bulk chemical composition. Bulk composition analyses were conducted at the University of Tennessee by wavelength X-ray fluorescence (XRF) Philips Magix Pro system. The XRF analyzes for major, minor, and trace elements. The XRF data was reported for major elements in weight percent and minor elements in ppm (parts per million) (Table B-1). Pressed pellets were made for each sample using 4 g of powdered sample and 5 g of boric acid. The XRF diagnostic procedure applied the appropriate limestone and shale standards. The calibration used was CALSOILS_091503 provided by the University of Tennessee.

CHAPTER IV

PETROGRAPHY OF MARBLES

Mineral assemblages in the analyzed samples are given in Table B-2 and their distribution in Figure A-4. The progressive contact metamorphism of the limestone resulted in the formation of tremolite and diopside. The marble samples are separated into three groups on the basis of their mineral assemblages. The first group includes samples containing neither tremolite nor diopside (unmetamorphosed-low grade). The second is defined by the presence of tremolite (tremolite zone). The third is defined by the presence of diopside (diopside zone).

Mineral and bulk compositions of these marble samples can be sufficiently characterized by the CaO-MgO-SiO₂-H₂O-CO₂ system. Mineral and bulk compositions can be projected from H₂O and CO₂ onto the CaO-MgO-SiO₂ plane (Figure A-5). This can be done as long as H₂O and CO₂ behave as boundary value components with chemical potentials that are independent variables during metamorphism.

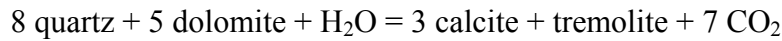
Low Grade Marbles

Low grade marble samples such as 29, 31, 38, 39, 40b, 50, 69, SC07, and SC08 show no remnants of original sedimentary or diagenetic textures. All of these samples show some type of foliated texture or deformation. The mineral assemblages present in these samples include calcite + quartz, calcite + quartz + dolomite, and quartz + dolomite. Calcite and dolomite grains in most samples are

altered and are very fine grained with grain sizes ranging from 0.8 mm – 2.0 mm. Quartz grains are found both in the matrix (~0.5 mm) and in veins. The quartz grains within the veins are much larger (1.0 mm – 2.0 mm) and appear to be unaltered. Graphite is present in many of the samples as foliated, scaly bands.

Tremolite Zone Marbles

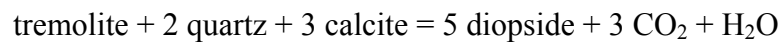
These samples are characterized by the appearance of tremolite by the reaction:



Examples of this assemblage include 17a, 49, 53, 60, 62a, and 71. These marbles also show signs of regional deformation with no relic sedimentary or diagenetic textures being preserved. All of these samples show some type of foliated texture or deformation. Mineral assemblages in these samples include calcite + dolomite + tremolite, calcite + quartz + tremolite, and calcite + tremolite. Tremolite occurs as prismatic blades (0.4 mm – 2.0 mm) and rhombic cross sections (0.5 mm). Some grains contain small fluid inclusions. Calcite grains (0.1 mm – 2 mm) are very similar to those in the unmetamorphosed samples. They are deformed and some have inclusions. Quartz (<0.1 mm) is a minor constituent in most of the samples, except for 62a where it is a major matrix component. Graphite is present in many of the samples as foliated, scaly bands.

Diopside Zone Marbles

These marble samples are marked by the appearance of diopside and the disappearance of tremolite represented by the reaction:



Examples of this zone include 8b, SCK03, and SCK06. The mineral assemblage present is calcite + quartz + diopside + muscovite + magnetite. Calcite grains are typically 0.1 mm – 3.0 mm with many of the larger grains containing diopside inclusions. Quartz grains are typically very small (0.1 mm - 0.5 mm) and make up a large portion of the matrix. Diopside grains are mostly prismatic with size ranging from 0.1 mm to 2.5 mm. Muscovite grains range in size from 0.1 mm to 1.0 mm. Magnetite grains typically range in size from 0.1 mm to 2.0 mm. Graphite is present in some of the samples as foliated, scaly bands.

CHAPTER V

TEMPERATURE AND FLUID COMPOSITION

Figure A-6 is a T-X (CO₂) diagram of the CaO-MgO-SiO₂-H₂O-CO₂ system at 4 kbar. The pressure of 4 kbar was estimated by the amount of overburden (12 km). This is the estimated thickness of the Paleozoic succession in Nevada (Pluijm and Marsh, 1997). The amount of overburden had to be estimated because of the deformation of the units in this area. Fluid compositions and temperatures were estimated in relation to invariant points 1 and 2. The estimated fluid composition was between X (CO₂) = 0.25 and 0.85. The temperature ranges for the tremolite isograd ranges from 450 to ~560°C. The temperature range for diopside isograd is between ~560 and ~565°C. This indicates metamorphism occurred between 450 and 565°C.

Figures A-7 and A-8 are T-X_{CO₂} diagrams of the CaO-MgO-SiO₂-H₂O-CO₂ system at 1 and 2 kbar. These diagrams show how temperatures and fluid compositions are affected by pressure. This was done because the overburden in this area is very difficult to determine because of the amount of deformation of the Harkless, Toquima formations, and an unnamed Paleozoic limestone unit. Shaw (2004) estimated the thickness of each unit to be several hundred meters.

The fluid composition is estimated to have been between X (CO₂) = 0.5 and 0.9 at 1 kbar. The temperature for the tremolite isograd ranges from 400 to 450 °C and the temperature for the diopside isograd ranges from 450 to 465 °C. This indicates metamorphism occurred between 400°C and 465°C. The estimated range of fluid composition is between X(CO₂)= 0.65 and 0.98 at 2 kbar. The

temperature range is from 475 to 525 °C for the tremolite isograd and from 525 to 550 °C for the diopside isograd. This indicates the temperatures for metamorphism range from 475 to 550 °C at 2 kbar. The difference in temperatures and fluid compositions between the diagrams (Figures A-6, A-7 and A-8) show how temperature and fluid compositions are affected by pressure. Therefore, temperature of metamorphism could range from 400 to 565 °C and fluid compositions between $X(\text{CO}_2) = 0.25$ and 0.98 for pressures between 1 kbar and 4 kbar.

CHAPTER VI MASS BALANCE

Mass Balance Calculations

The amounts of metamorphic phases, original phases, CO₂, and H₂O are determined by using mass-balance equations. This is done presuming that metamorphism was isochemical. Mass balance was determined for the transition from an unmetamorphosed limestone assemblage to a metamorphosed limestone assemblage. Cation fractions were normalized to 100.0 and calculated into an assemblage of unmetamorphosed assemblage and into a metamorphosed assemblage. The calculations are the same as used by Labotka (1984). In matrix notation the mass balance calculations were computed as $\mathbf{x} = \mathbf{A}\mathbf{y}$. \mathbf{x} is a vector indicating the rock composition, \mathbf{y} is a vector denoting the abundance of minerals, and \mathbf{A} is a matrix including the compositions of each mineral. In the situation where the number of minerals is less than the number of components, $\mathbf{y} = (\mathbf{A}^\dagger \mathbf{A})^{-1} \mathbf{A}^\dagger \mathbf{x}$. The chi-square test statistic $\chi^2 = \sum_i [(x_i - \bar{x}_i)^2 / \bar{x}_i]$, in which x_i is the determined amount of cation i , and \bar{x}_i is the real value, is the measure of the goodness-of-fit of the least-squares estimate (Labotka et al. 1984). In most cases, the number of minerals is equivalent to the number of components $\chi^2 \approx 0$.

The first step is to calculate the amount of phases in the rock sample from 10 metamorphosed samples (Table B-3). This is done by calculating the amounts of CaO, MgO, and SiO₂ from the bulk chemical analysis. The data were converted to moles from weight percent. Then using mass balance equations the

relative abundance of the metamorphic phases was then determined. This is the mineral abundance after metamorphism seen in Table B-3. The amounts of calcite and dolomite represent the amount of CO₂ in the sample. Therefore, the amount of CO₂ was determined from mass balance calculations. Tremolite (Ca₂Mg₅Si₈O₂₂(OH)₂) was used to indicate the amount of H₂O in the sample.

The second step is to calculate the original mineral abundance of the rock. This is done assuming the original limestone is composed of only calcite, dolomite, and quartz. The data were again converted from weight percents into moles. Then original phase amounts were determined using the mass balance equation. CO₂ amounts were determined by the abundance of calcite and dolomite.

Determining Changes in Volume and CO₂

The final step includes determining the change in CO₂ and the change in volume. The change in CO₂ is determined by the difference in CO₂ content in the before and after assemblages (Table B-3). The change in volume is found by calculating the volume of each phase in both before and after assemblages. The calculation of volume was accomplished by converting the number of moles of each phase into volume (cm³). The sum of the phase volumes represents the total volume of that particular sample. 1 kg of mass was the basis for the calculation.

The results in Table B-3 show there is a difference in the change in CO₂ and volume values. Figure B-9 shows the change in volume versus distance from the contact. The plot shows a decrease in the change in volume with increasing distance. This demonstrates how metamorphic processes affected the amount of

CO₂ in these limestones. The greater the metamorphic grade the greater the loss of CO₂.

CHAPTER VII

BULK CHEMISTRY

Testing the assumption of isochemical metamorphism is difficult in the absence of mineralogical evidence for metasomatism. Variations in bulk compositions among the low grade metamorphosed marbles and the higher grade marbles can be the result of differences in the bulk compositions of the protoliths, such as the Zanzibar and the Toquima. The weight ratios of various oxides to Al_2O_3 are arranged by increasing distance from the contact (Figure A-10). Aluminum is believed to be an immobile element, and changes in the ratios could show changes in bulk compositions during metamorphism (Labotka et al. 1984). This figure shows increases in major elements, except for K_2O , with increasing metamorphic grade. This is most likely due to chemical differences in the stratigraphic units. For example, the first two samples, SCK03 and SCK06, have a different mineral assemblage (diopside + quartz + calcite + muscovite + magnetite) compared with the other samples (calcite + dolomite + quartz and tremolite + calcite + quartz). The increased values in Na, Si, and Fe are due to the presence of muscovite and magnetite.

CHAPTER VIII STABLE ISOTOPES

Zanzibar Isotopic Data

This study looked at $\delta^{18}\text{O}$ and $\delta^{13}\text{C}$ values for calcite and dolomite samples to determine if there are any patterns resulting from the emplacement of the pluton. The first step is to look at the $\delta^{18}\text{O}$ and $\delta^{13}\text{C}$ values for calcite in 20 samples located throughout the study area. Zanzibar and Toquima $\delta^{18}\text{O}$ and $\delta^{13}\text{C}$ values are shown in Table B-4 and the distributions of values are shown in Figures A-11 and A-12. Figure A-13 shows $\delta^{18}\text{O}$ versus distance from the contact for both Zanzibar and Toquima samples. This plot shows no correlation between increasing distance and increasing oxygen isotopic values for Zanzibar samples. Isotopic compositions also vary when it comes to metamorphic grade. For example, many of the diopside bearing samples have high values (~19.0-21.0‰) and some of the low grade samples have very low values (~11.0-13.0‰) (Figure A-9 and Table A-4). Figure A-14 shows $\delta^{13}\text{C}$ versus distance from the pluton. This plot shows no systematic decrease in $\delta^{13}\text{C}$ with decreasing distance from the pluton.

The second step was to look at Zanzibar samples that contain dolomite. The values for $\delta^{18}\text{O}$ and $\delta^{13}\text{C}$ can be seen in Table B-5 and the distributions of values are shown in Figures A-15 and A-16. Figures A-13 and Figure A-14 show oxygen and carbon isotopic values of dolomite versus distance from the contact. These plots show similar results to that of calcite. The oxygen values show no

increase with increasing distance. The carbon values show no pattern of increase with increasing distance.

Toquima Isotopic Data

Toquima calcite $\delta^{18}\text{O}$ and $\delta^{13}\text{C}$ values are shown in Table B-4 and the distributions of values are shown in Figures A-11 and A-12. Figure A-13 shows $\delta^{18}\text{O}$ versus distance from the contact for both Zanzibar and Toquima samples. This plot shows $\delta^{18}\text{O}$ values increasing with increasing distance from the pluton. Figure A-14 shows $\delta^{13}\text{C}$ versus distance from the pluton. Carbon isotope values also increase with increasing distance from the pluton. Dolomite $\delta^{18}\text{O}$ and $\delta^{13}\text{C}$ values are shown in Table B-5 and the distributions of values in Figures A-15 and A-16. Figures A-13 and Figure A-14 show oxygen and carbon isotopic values of dolomite versus distance from the contact. These plots show similar results to that of calcite. Therefore, oxygen and carbon isotope values appear to be systematic with distance from the pluton.

Comparison of Zanzibar and Toquima Isotope Values

Figure A-19 shows a plot of $\delta^{18}\text{O}$ vs. $\delta^{13}\text{C}$ values for Zanzibar and Toquima samples. Oxygen values are widely distributed among both Zanzibar and Toquima samples. Zanzibar samples range between ~15.0‰ and 25.0‰ and Toquima samples between ~11.0‰ and 23.0‰. There is an observed difference in carbon values between the Zanzibar and Toquima. Zanzibar sample values seem to be lower than values for Toquima samples (Figures A-14 and A-19). This indicates the Zanzibar formation carbon values were more influenced by metamorphism. Figure A-19 also shows values samples containing both

dolomite and calcite. These samples show consistently lower carbon and oxygen values for calcite than dolomite. This indicates calcite was more influenced by metamorphic activity.

Comparison of Calcite and Dolomite Oxygen Isotopic Data

Figure A-18 is a plot of $\delta^{18}\text{O}$ values of calcite vs. dolomite. This plot shows a trend of calcite vs. dolomite oxygen values close to 1/1 indicating they are at equilibrium. These values also plot between the 300°C and 25°C fractionation lines. This indicates these samples fractionated at temperatures below 300°C and above 25°C.

CHAPTER IX DISCUSSION

Declining values in $\delta^{18}\text{O}$ and $\delta^{13}\text{C}$ have been noticed in contact metamorphosed calc-silicate rocks at several locations discussed by Valley (1986). Two examples are the contact metamorphosed calcareous argillites of the Big Horse Member (Nabelek et al. 1984) and regionally metamorphosed calc-silicates of the Valley Spring Gneiss, Texas (Bebout and Carlson, 1986). Both cases show decreases in $\delta^{13}\text{C}$ and $\delta^{18}\text{O}$. In general, these studies indicate that lower $\delta^{13}\text{C}$ values can be explained by Rayleigh decarbonation, but the decreases in $\delta^{18}\text{O}$ cannot be explained by decarbonation.

Carbon Isotopes

The $\delta^{13}\text{C}$ values for Toquima calcite and dolomite show decreasing values with decreasing distance from the pluton. These declining values are indicative of contact metamorphism. This same pattern is not seen in Zanzibar samples. Figure A-19 shows Zanzibar $\delta^{13}\text{C}$ values of calcite versus the fraction of CO_2 remaining after metamorphism. This plot shows most carbon values falling in or near the envelope defined by Rayleigh and batch decarbonation. This indicates Zanzibar $\delta^{13}\text{C}$ values for calcite are more systematic with reaction than with distance from the pluton.

Oxygen Isotopes

Oxygen Isotope Values and Change in Volume

The $\delta^{18}\text{O}$ values for calcite and dolomite in Toquima samples show decreasing values with decreasing distance from the pluton. Again, these

declining values are indicative of contact metamorphism. The $\delta^{18}\text{O}$ values for Zanzibar calcite and dolomite show no evidence they were affected by metamorphic reactions. Figure A-20 shows the comparison of the change in volume vs. $\delta^{18}\text{O}$ values. Figure A-21 is a plot of $\delta^{18}\text{O}$ values versus the remaining fraction of CO_2 . These plots show no evidence of $\delta^{18}\text{O}$ values being affected by decarbonation. Therefore, Zanzibar $\delta^{18}\text{O}$ values are not corresponding to typical patterns associated with contact metamorphism.

Alteration of Oxygen Isotope Values

The main possibility of altered Zanzibar $\delta^{18}\text{O}$ values is the formation of ore deposits during volcanic activity in the Tertiary. Samples analyzed using cathodoluminescence shows evidence for secondary calcite and luminescence along grain boundaries (Figure A-22). This indicates these rocks came into contact and exchanged with some type of fluid after these rock were metamorphosed by the emplacement of the Belmont pluton (Houzar, 2003).

Taylor (1974) stated igneous intrusions emplaced into permeable country rocks act as gigantic heat engines that set up long lived hydrothermal convection. This process then continues through the cooling and crystallization of the intrusion. He also stated the majority of the magmatic water is small compared with the large amount of heated meteoric ground water. In the area of Tonopah, Nevada (~50 miles southwest of Belmont), Taylor found alteration zones were formed by these low oxygen isotopic meteoric fluids (Taylor, 1974). These meteoric fluids are more than likely the cause of the altered oxygen isotopic values.

CHAPTER X

CONCLUSION

The mineral assemblages of the Zanzibar formation and Toquima formation are characterized by the appearances of tremolite and diopside. The formation of these assemblages indicates the temperature of metamorphism was between 400 – 565°C (Figures A-6, A-7, and A-8). The fluid composition was estimated to be between 0.25 and 0.98 (Figures A-6, A-7, and A-8). This indicates the fluid was mostly CO₂ rich and there was no significant contribution of water from the pluton.

Stable isotope data show carbon values decreasing with increasing distance from the contact for Toquima samples and Zanzibar carbon values are systematic with extent of reaction (Figures A-14 and A-19). Oxygen isotopic values for Toquima samples correspond to distance to the contact, but Zanzibar samples do not (Figure A-13). Zanzibar oxygen isotope values also do not correspond to extent of reaction (Figure A-21). This indicates they have been altered after the intrusion of the pluton. The alteration of these values most likely resulted from contact with fluids derived during volcanic activity in the Tertiary.

LIST OF REFERENCES

LIST OF REFERENCES

- Baumgartner, L.P. and Valley, J.W. (2001) Stable isotope transport and contact metamorphic fluid flow. *Reviews in Mineralogy*. 43, 415-461.
- Bebout, G.E. and Carlson, W.D. (1986) Fluid evolution and transport during metamorphism: evidence from the Llano Uplift, Texas. *Contributions to Mineralogy and Petrology*. v. 92, pp. 518-529.
- Bergfeld, D., Nabelek, P.I., and Labotka, T.C. (1996) Carbon isotope exchange during polymetamorphism in the Panamint Mountains, California, USA. *Journal of Metamorphic Geology*. v. 14, pp. 199-212.
- DeCelles, P.G. (2004) Late Jurassic to Eocene evolution of the Cordilleran thrust belt and foreland basin system, Western U.S.A. *American Journal of Science*. v. 304, pp. 105-168.
- Ferry, J.M. (1991). Dehydration and Decarbonation Reactions as a Record of Fluid Infiltration. *Reviews in Mineralogy*. v. 26. pp. 351-393.
- Hover-Granath, V.C., Papike, J.J., and Labotka, T.C. (1983) The Notch Peak contact metamorphic aureole, Utah: Petrology of the Big Horse limestone member of the Orr Formation. *Geologic Society of America Bulletin*. v. 94, pp. 889-906.
- Houzar, S., and Leichmann, J. (2003). Application of cathodoluminescence to the study of metamorphic textures in marbles from the eastern part of the Bohemian Massif. v. 78, pp. 241-250.
- Labotka, T.C., White, C.E., and Papike, J.J. (1984) The evolution of water in the contact-metamorphic aureole of the Duluth Complex, northeastern Minnesota: *Geological Society of America Bulletin*, v. 95, p. 788-804.
- Nabelek, P.I. (1991) Stable Isotope Monitors. *Reviews in Mineralogy*. v. 26, pp. 395-430.
- Nabelek, P.I., Labotka, T.C., O'Neil, J.R., and Papike, J.J. (1984) Contrasting fluid/rock interaction between the Notch Peak granitic intrusion and argillites and limestones in western Utah: evidence from stable isotopes and phase assemblages: *Contributions to Mineralogy and Petrology*. v. 86, pp. 25-34.
- Nabelek, P.I., Hanson, G.N., Labotka, T.C., and Papike, J.J. (1988) Effects of fluids on the interaction of granites with limestones: Notch Peak Stock, Utah. *Contributions to Mineralogy and Petrology*. v. 99, pp. 49-61.

- Pluijm, B. A and Marsh, S. (1997) *Earth Structure: An introduction to structural geology and tectonics*. McGraw-Hill pp. 459-461.
- Shaw, D. R. (2002) *Geologic Map of part of the southern Toquima Range and adjacent area, Nye County, Nevada*. U.S. Geological Survey Miscellaneous Field Studies Map MF-2327-A. 1:48,000 scale.
- Sheild, G.A. (2003) Sr, C, and O isotope geochemistry of Ordovician brachiopods: A major isotopic event around the Middle-Late Ordovician transition. *Geochimica et Cosmochimica Acta*. v. 67, pp. 2005-2025.
- Sheppard, S.M.F. and Schwarcz, H.P. (1970) Fractionation of carbon and oxygen isotopes and magnesium between coexisting metamorphic calcite and dolomite. *Contributions to Mineralogy and Petrology*. v. 26, pp. 161-198.
- Spear, F.S. (1992) *Metamorphic Phase Equilibria and Pressure-Temperature-Time Paths*. Mineralogical Society of America.
- Taylor, H.P. (1974) The application of oxygen and hydrogen isotope studies to problems of hydrothermal alteration and ore deposition. *Economic Geology*. v. 69, pp. 843-883.
- Valley, J.M. (1986) Stable isotope geochemistry of metamorphic rocks In “Stable Isotopes in High Temperature Geologic Processes”, J.W. Valley, H.P. Taylor, J.R. O’Neil, Eds., *Reviews in Mineralogy*. v. 16, pp. 441-490.

APPENDICES

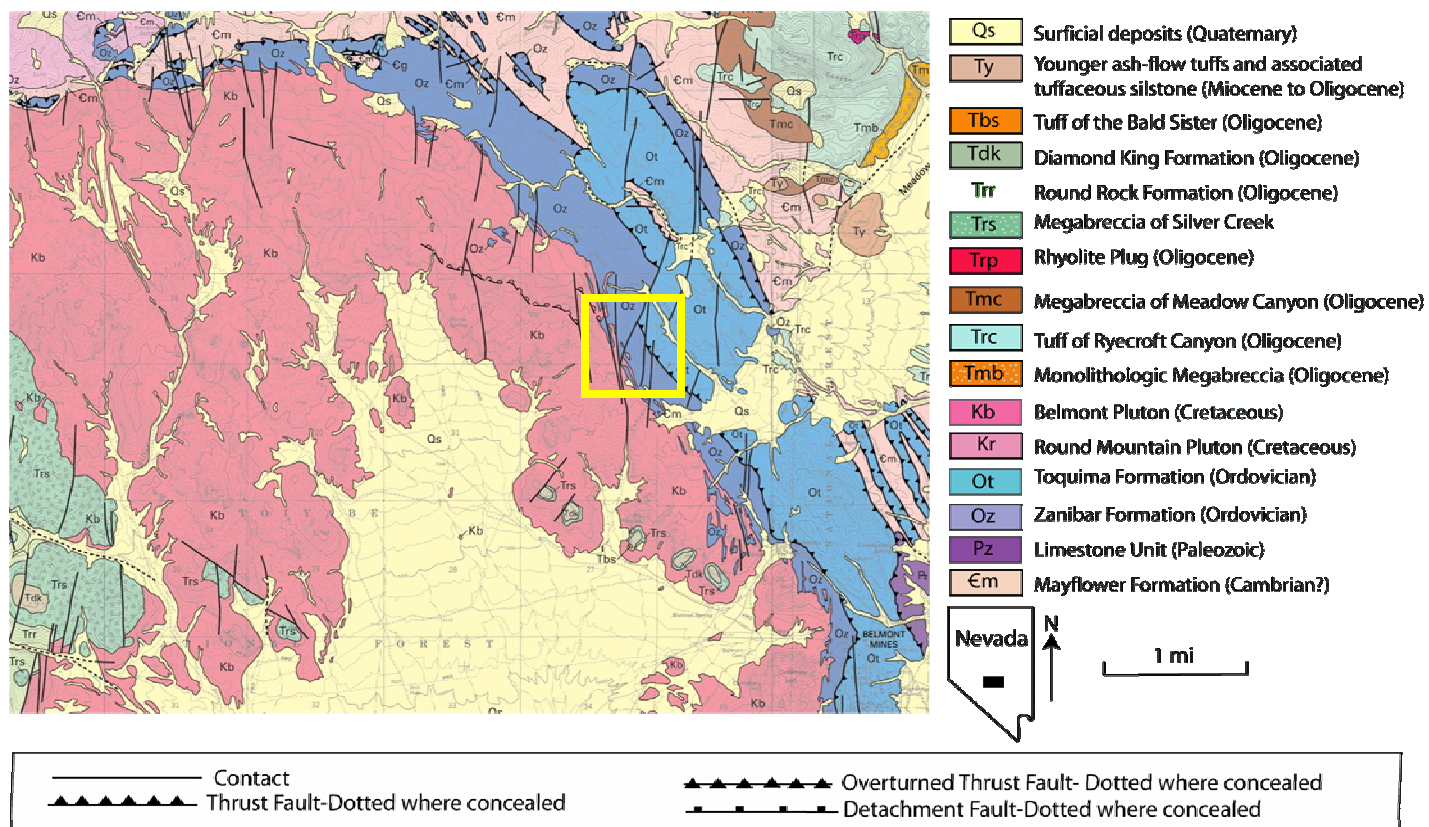


Figure A-1. Geologic map of Belmont area by Shaw, 2000. This map shows the locations of the Manhattan Caldera, Belmont pluton, Round Mountain pluton, the Zanzibar Formation, Toquima Formation, and the lower part of the Mount Jefferson caldera (Shaw, 2002). The yellow box indicates the field area.

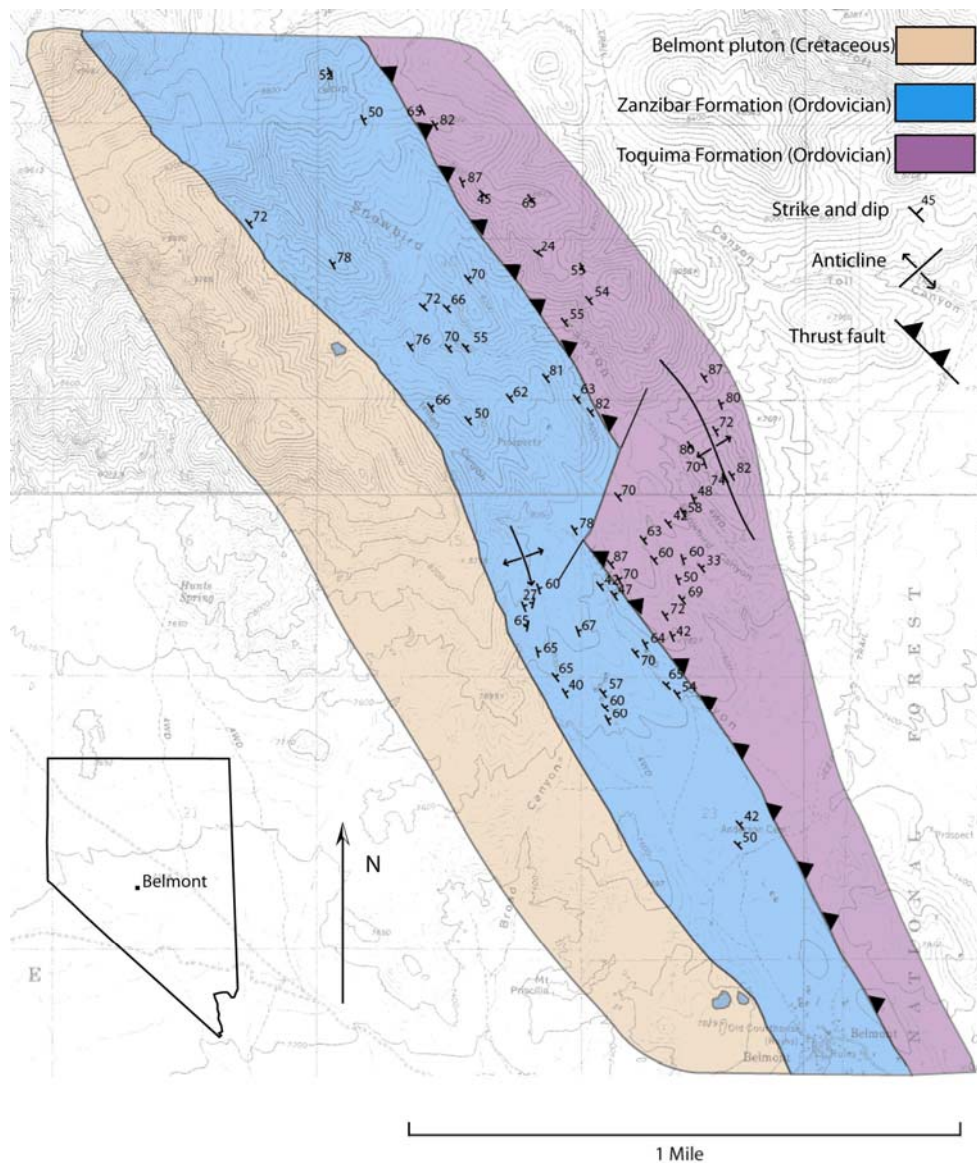


Figure A-2. Geologic map of field area. This map shows the geologic units(Zanzibar, Toquima, and Belmont) , structures, and strike and dip measurements.

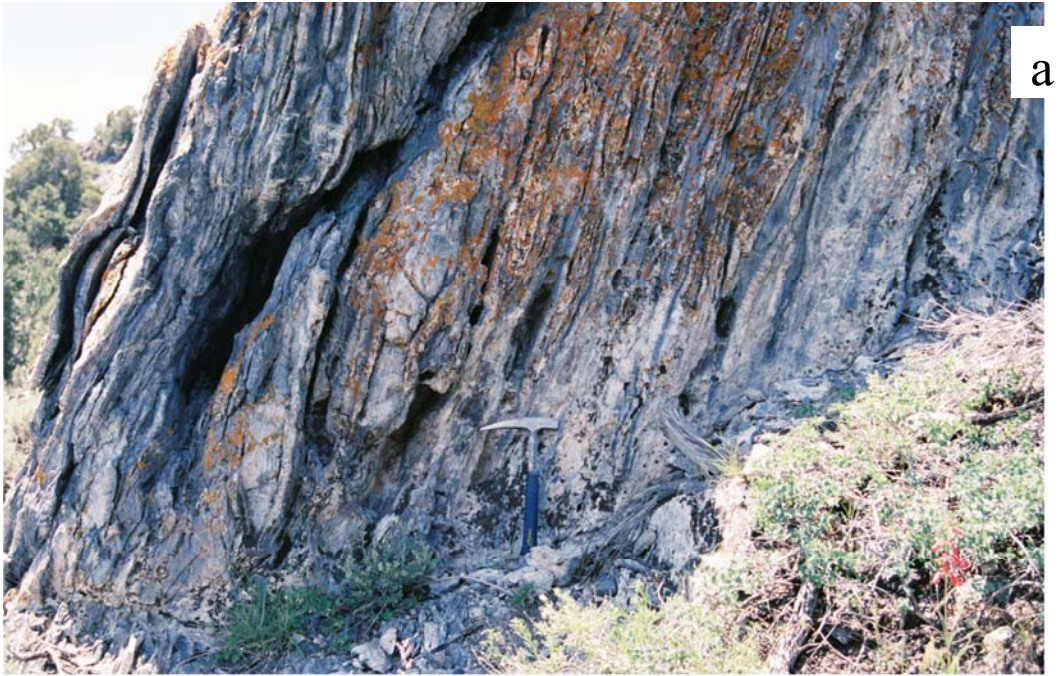


Figure A-3. Foliated marbles in the Zanzibar formation. Figure 3a shows tremolite and calcite veins parallel to the foliation. Figure 3b is an up close view of some of the tremolite veins within the Zanzibar.

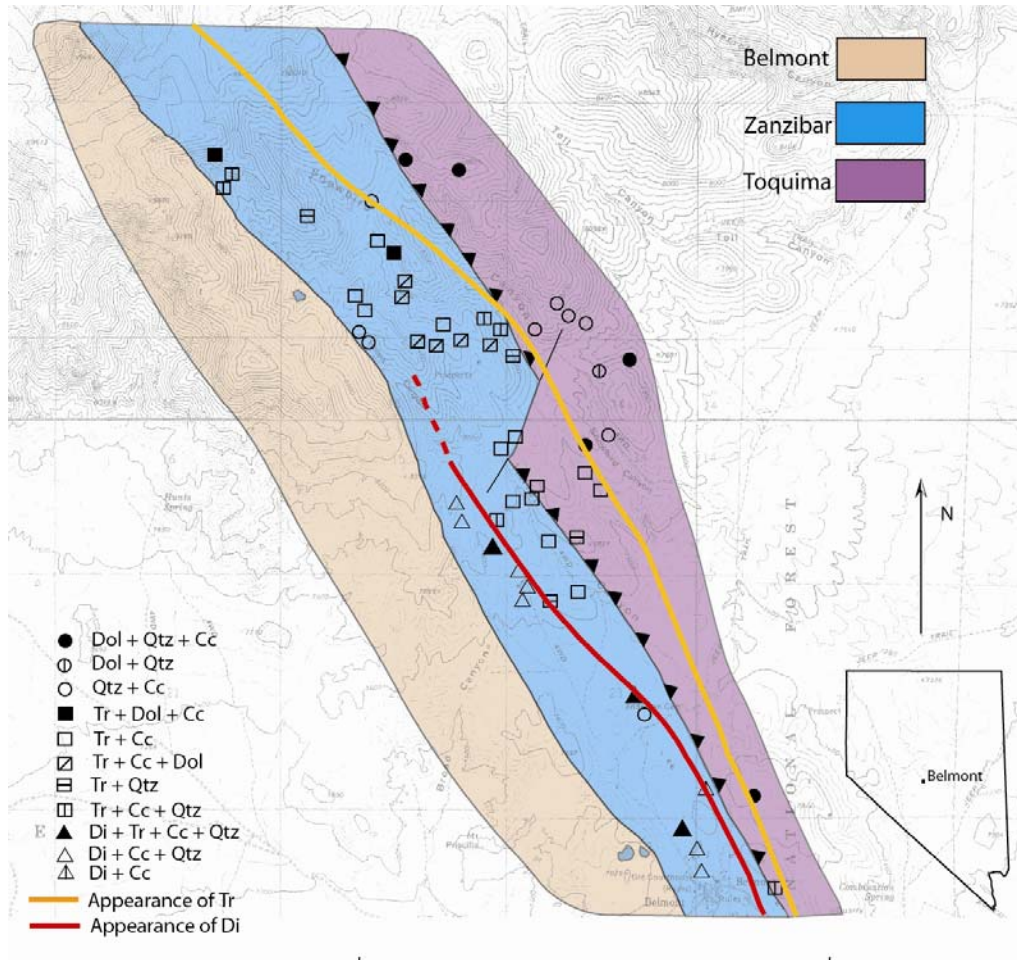


Figure A-4. Field map of sample distributions and mineral isograds.

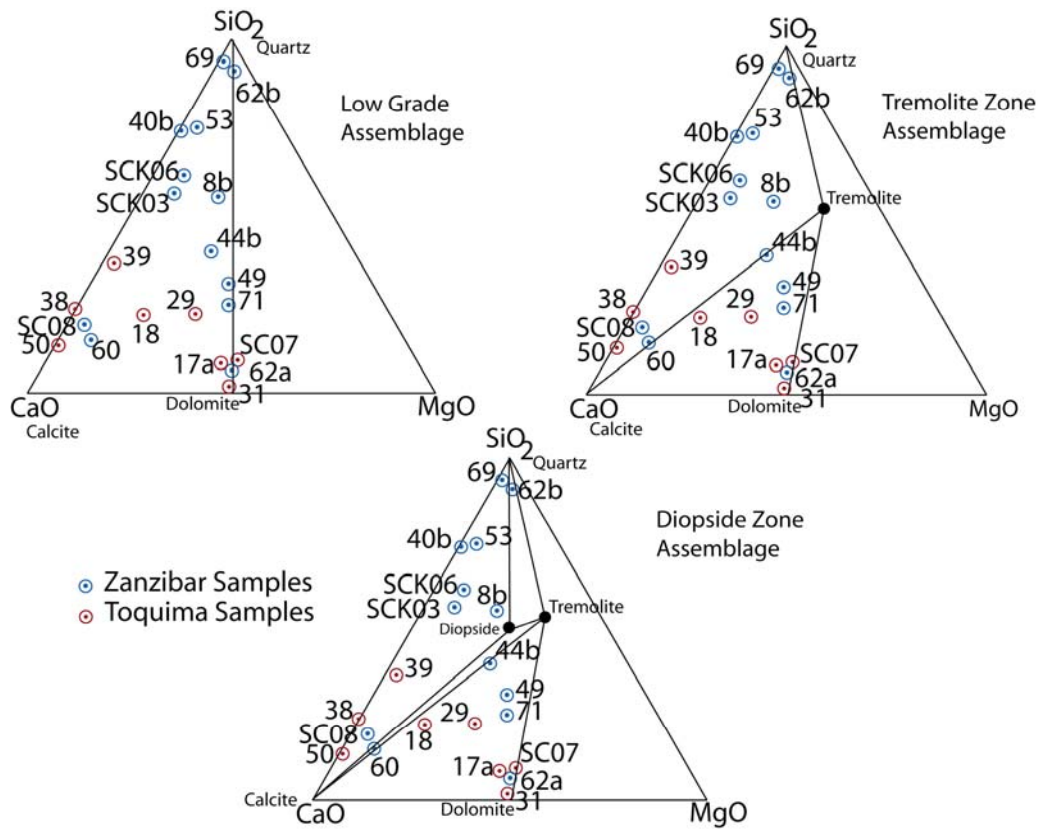


Figure A-5. Bulk composition of low grade, tremolite zone, and diopside zone assemblages projected on to the MgO-CaO-SiO₂ diagram. The blue sample points represent Zanzibar sample and the red sample points represent Toquima samples. This diagram shows the starting composition each sample and how increased metamorphic grade changes the assemblage. For example, 17a started out as the assemblage qtz + cc + dol, which later falls in the tr + cc + dol field for the tremolite and diopside zone assemblages. This correlates with the actual mineral assemblage of the sample.

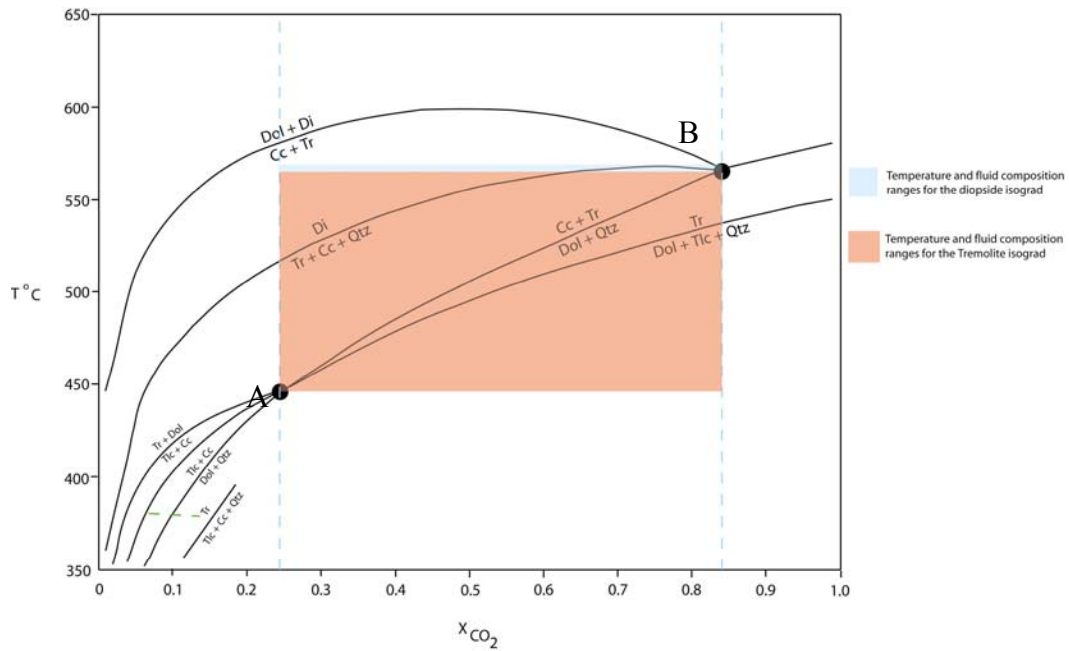


Figure A-6. T-X diagram for the CaO-MgO-SiO₂-H₂O-CO₂ system at 4 kbar calculated using Thermocalc. The pink color represents the ranges of fluid compositions (0.25-0.85) and temperature (450°C - 560°C) for the tremolite isograd. The blue color area represents the ranges of fluid composition (0.25-0.85) and temperature (560°C - 565°C) for the diopside isograd.

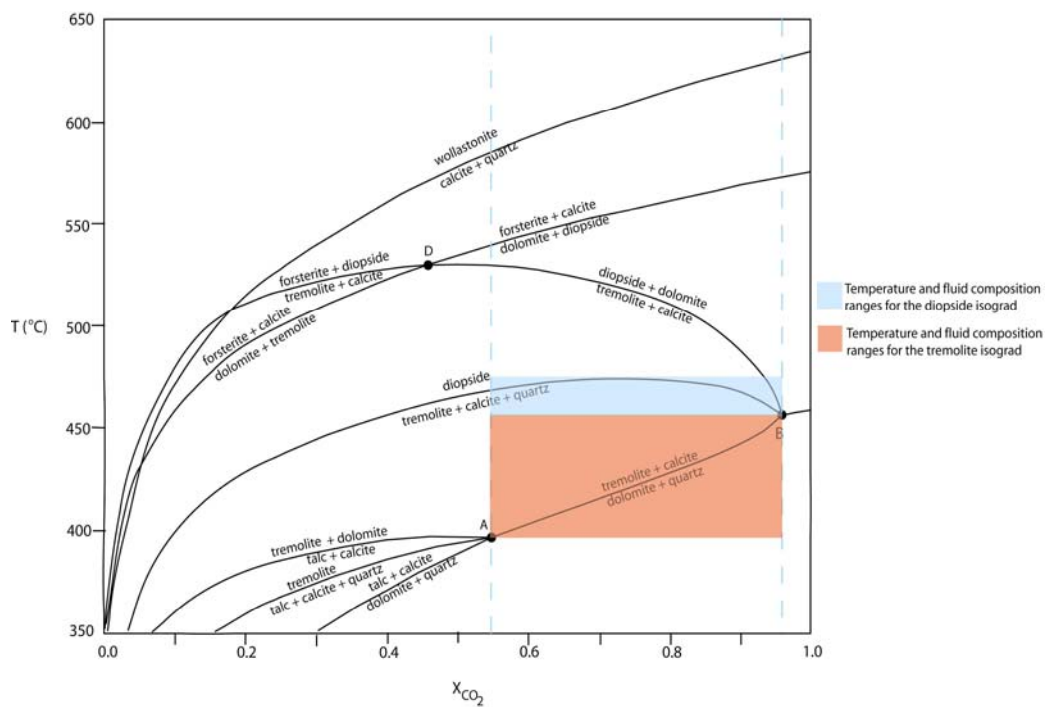


Figure A-7. T-X diagram for the CaO-MgO-SiO₂-H₂O-CO₂ system at 1 kbar calculated using Thermocalc. The pink color represents the ranges of fluid compositions (0.55-0.98) and temperature (400°C -450°C) for the tremolite isograd. The blue color area represents the ranges of fluid composition (0.55-0.98) and temperature (450°C -475°C) for the diopside isograd.

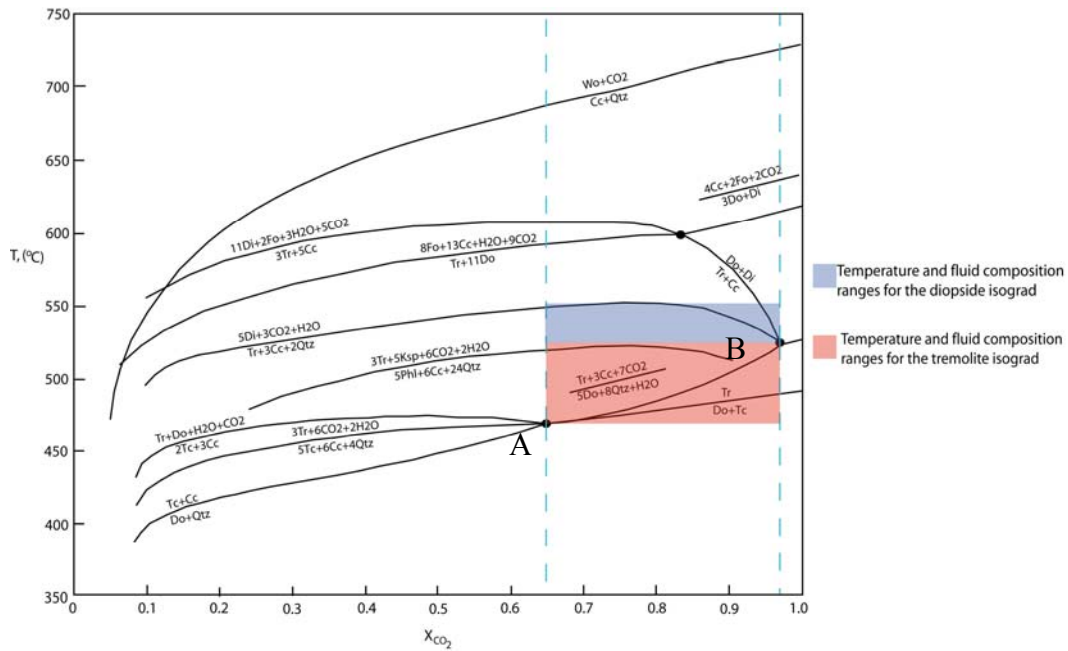


Figure A-8. T-X diagram for the CaO-MgO-SiO₂-H₂O-CO₂ system at 2 kbar, after Hover-Granath et al, (1983). The pink color represents the ranges of fluid compositions (0.65-.98) and temperature (475°C -525°C) for the tremolite isograd. The blue color area represents the ranges of fluid composition (0.65-0.98) and temperature (525°C -550°C) for the diopside isograd.

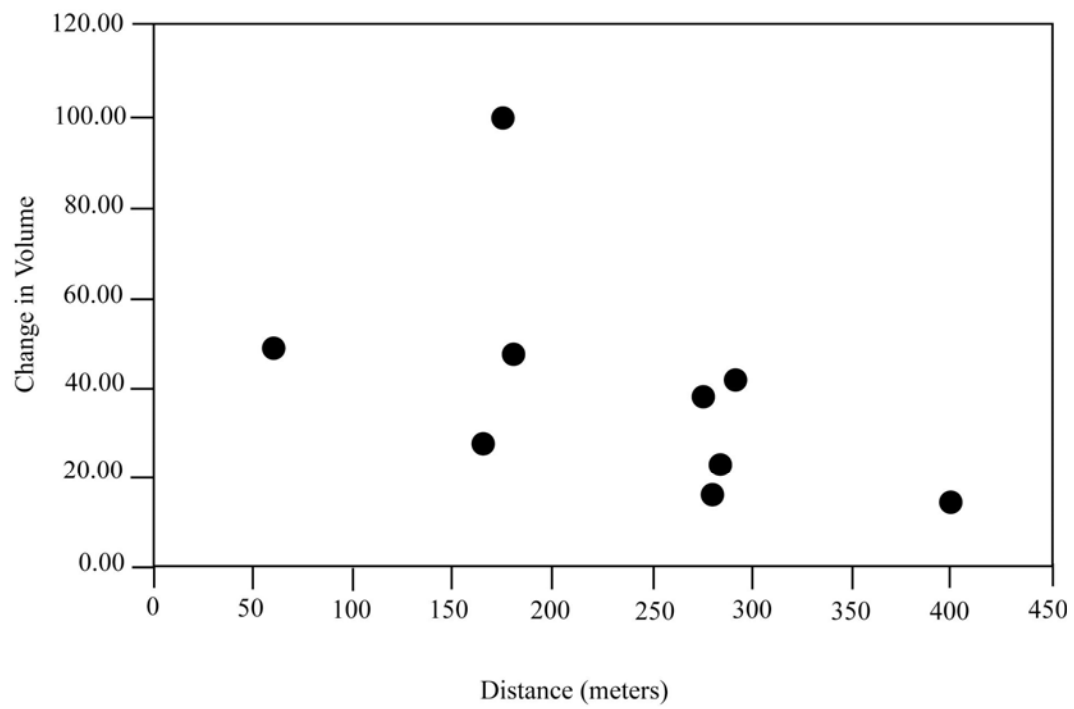


Figure A-9. Change in volume versus distance from the contact.

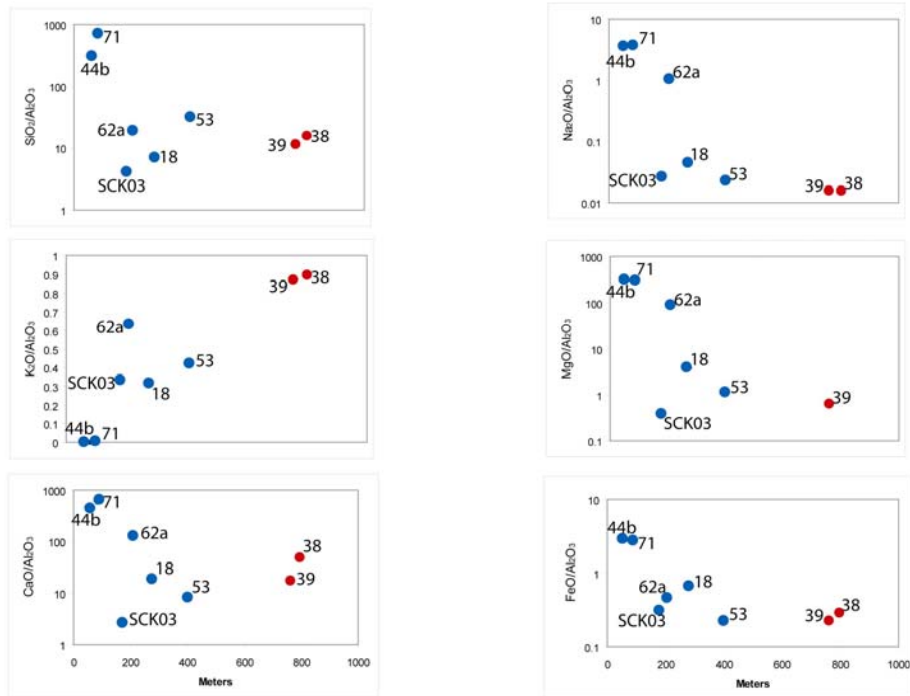


Figure A-10. Bulk compositions of 8 limestone samples from the Zanzibar (blue) and Toquima (red) formations determined by X-ray fluorescence. All values are expressed in weight percent ratios of various oxides to Al_2O_3 . Samples are given, left to right, in order of increasing distance from the contact.

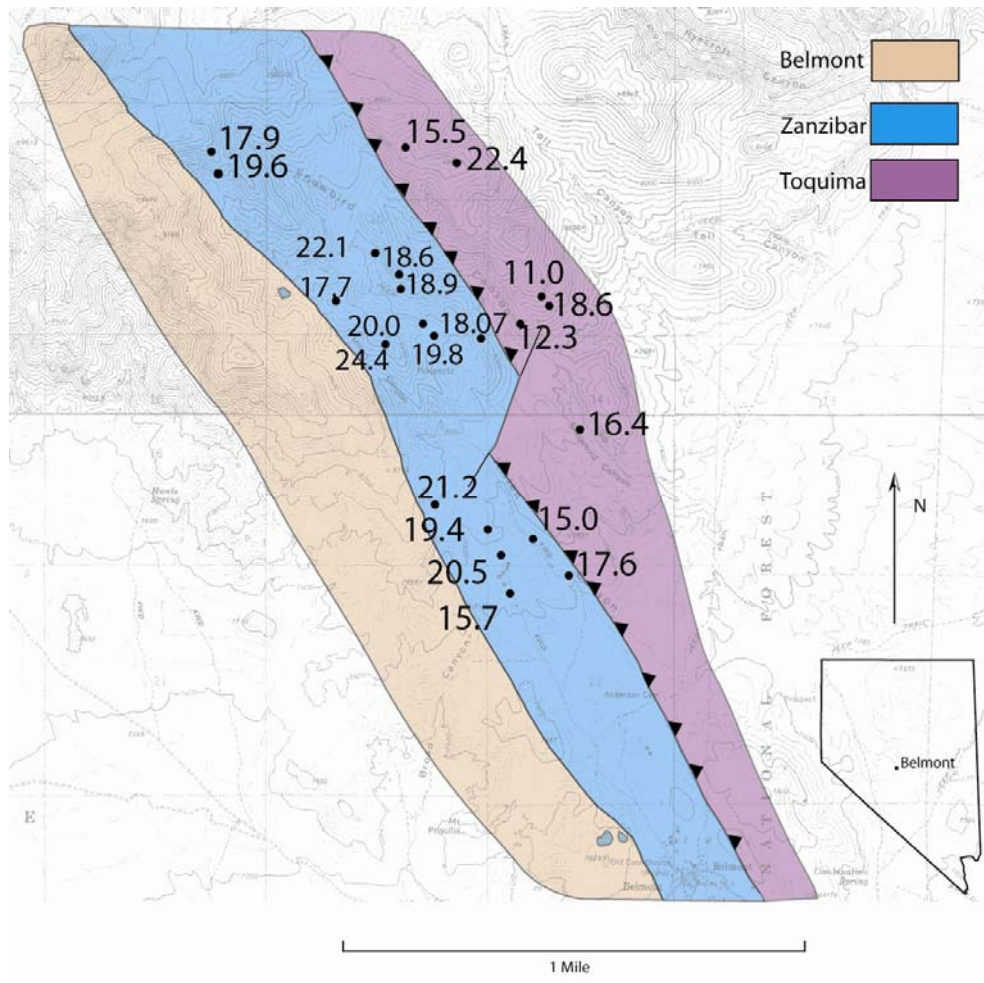


Figure A-11. Distribution of calcite $\delta^{18}\text{O}$ values (SMOW).

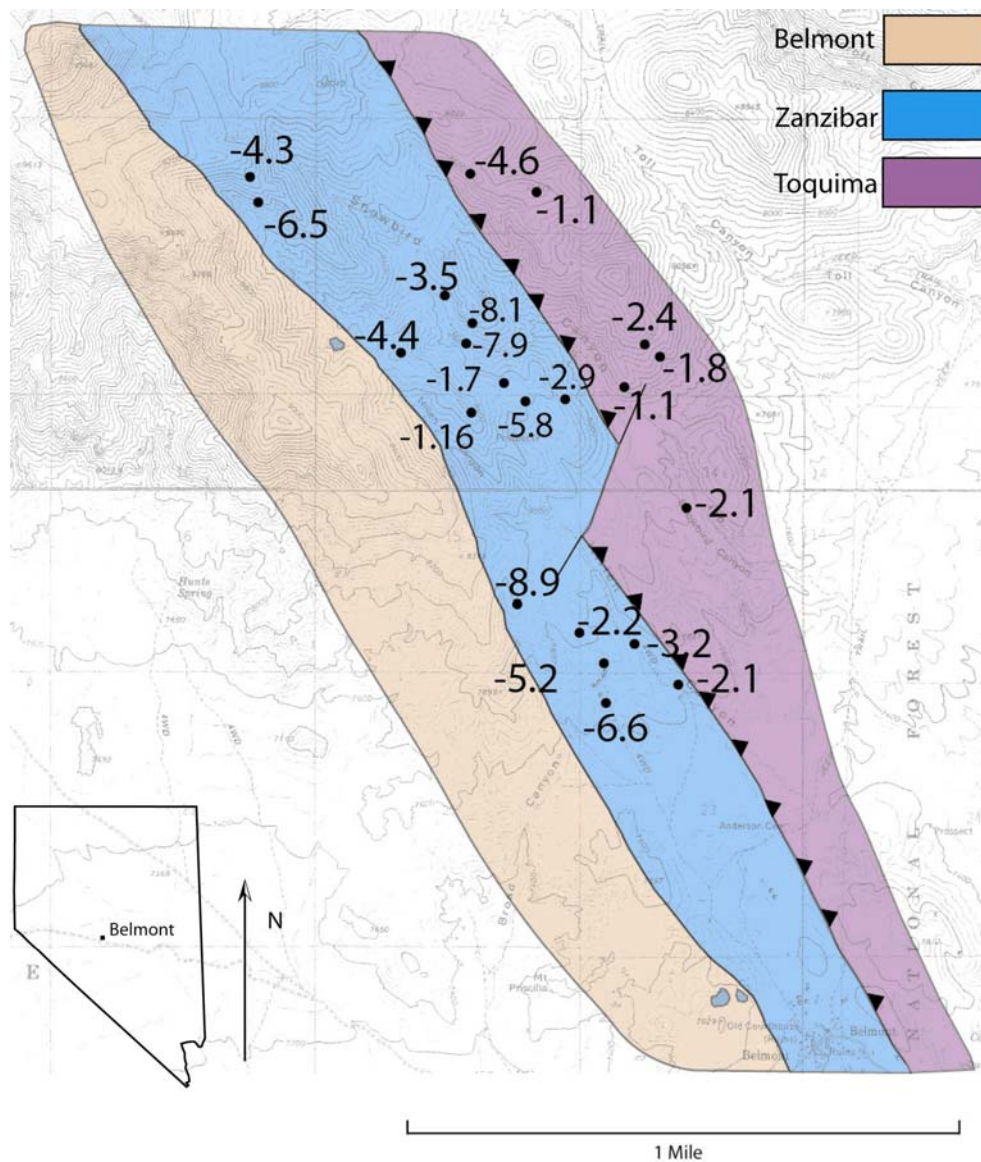


Figure A-12. Distribution of calcite $\delta^{13}\text{C}$ values (PDB).

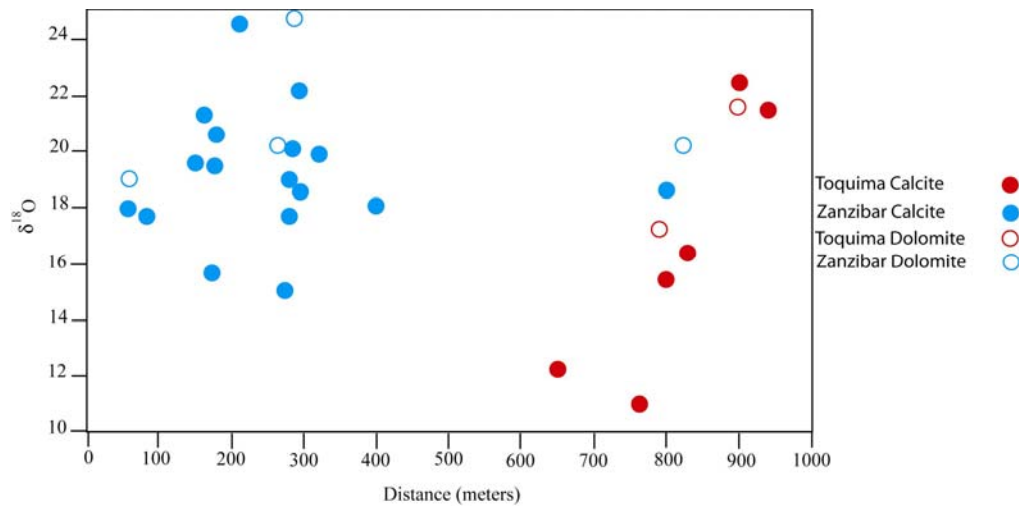


Figure A-13. Plot of $\delta^{18}\text{O}$ versus distance from the pluton.

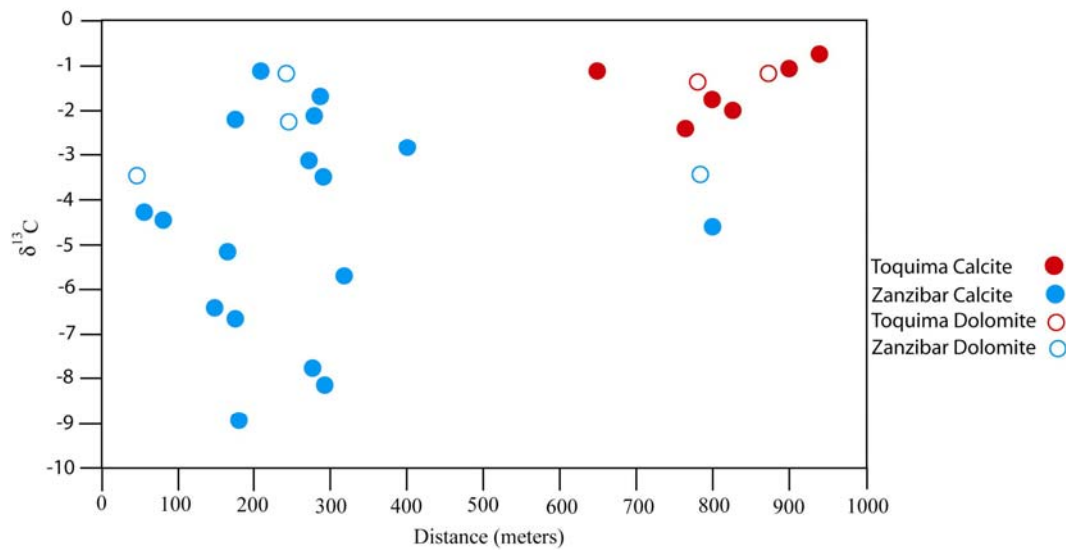


Figure A-14. Plot of $\delta^{13}\text{C}$ versus distance from the pluton.

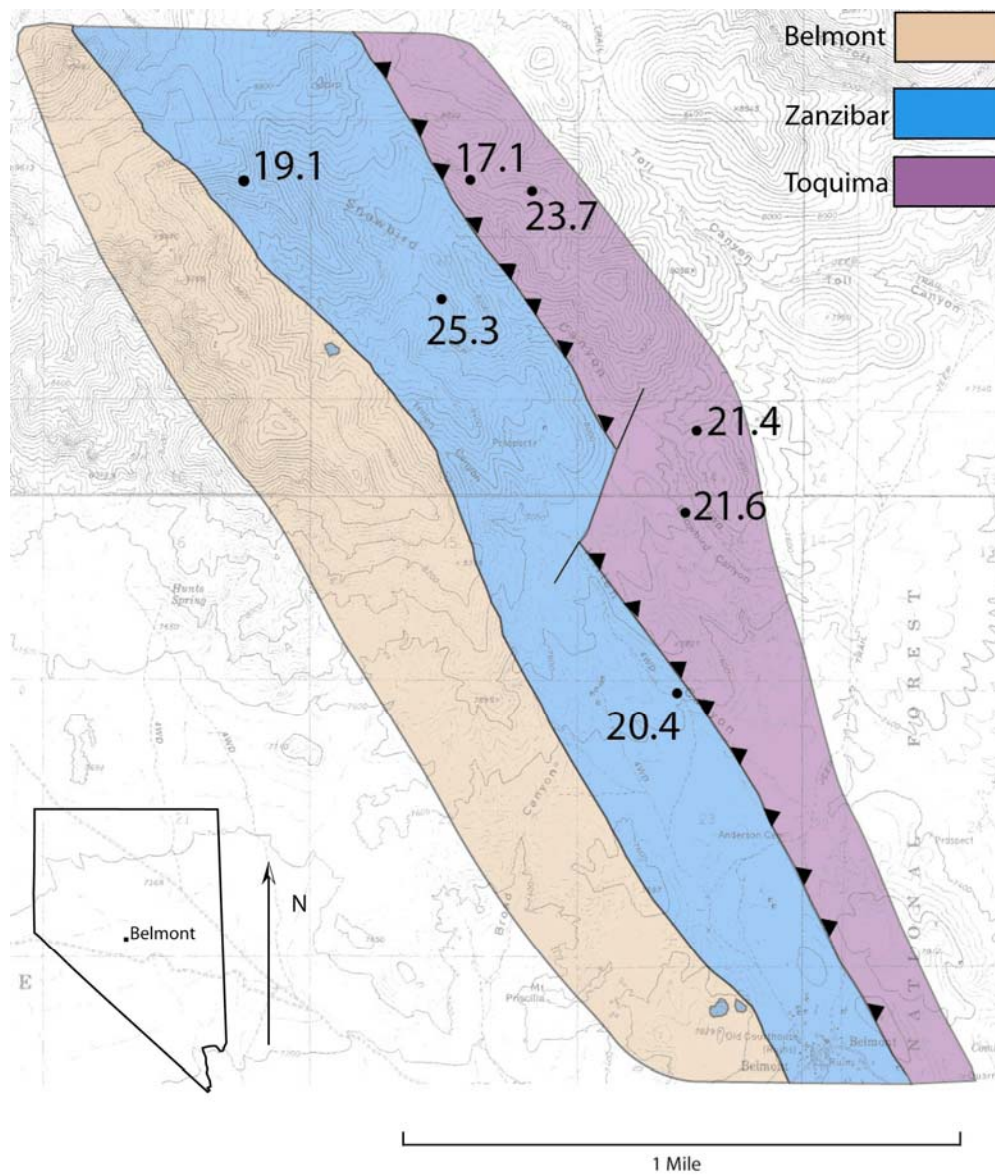


Figure A-15. Distribution of dolomite $\delta^{18}\text{O}$ values (SMOW).

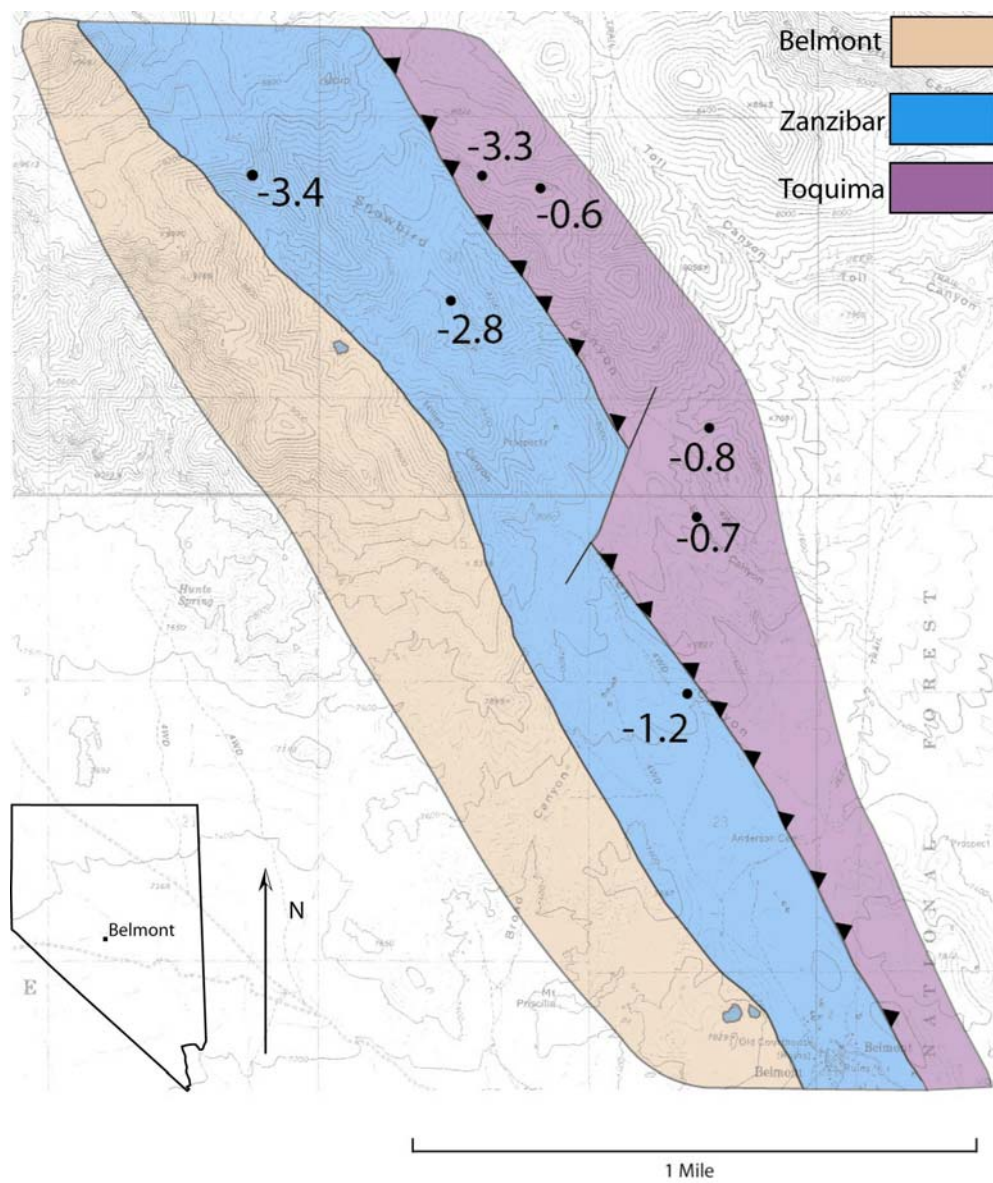


Figure A-16. Distribution of dolomite $\delta^{13}\text{C}$ values (PDB).

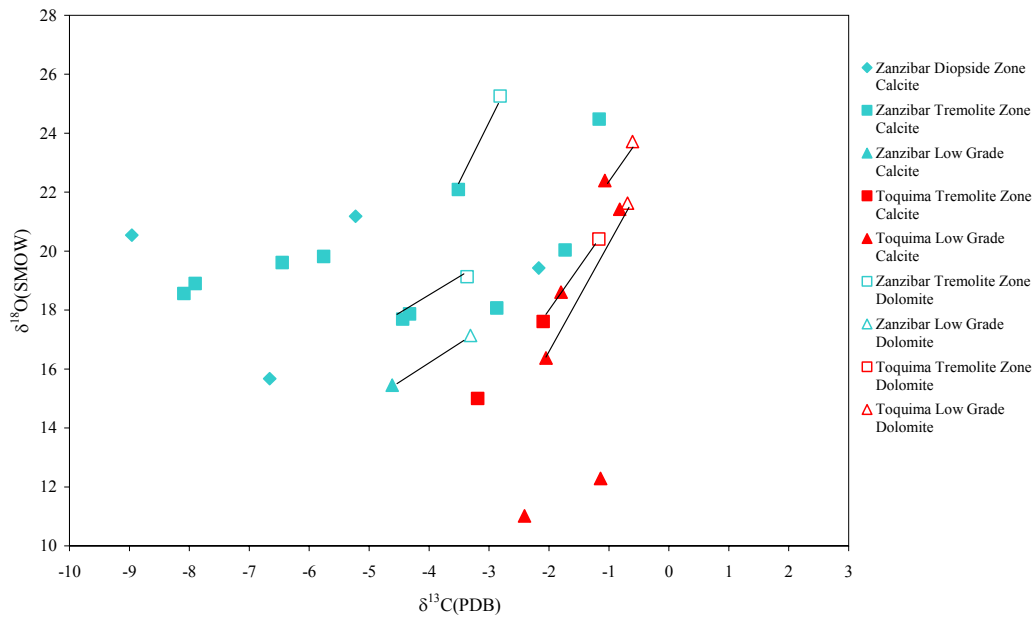


Figure A-17. Plot of $\delta^{18}\text{O}$ and $\delta^{13}\text{C}$ calcite and dolomite values for Zanzibar and Toquima marbles. Symbols represent metamorphic grade and the lines indicate calcites and dolomites within the same sample.

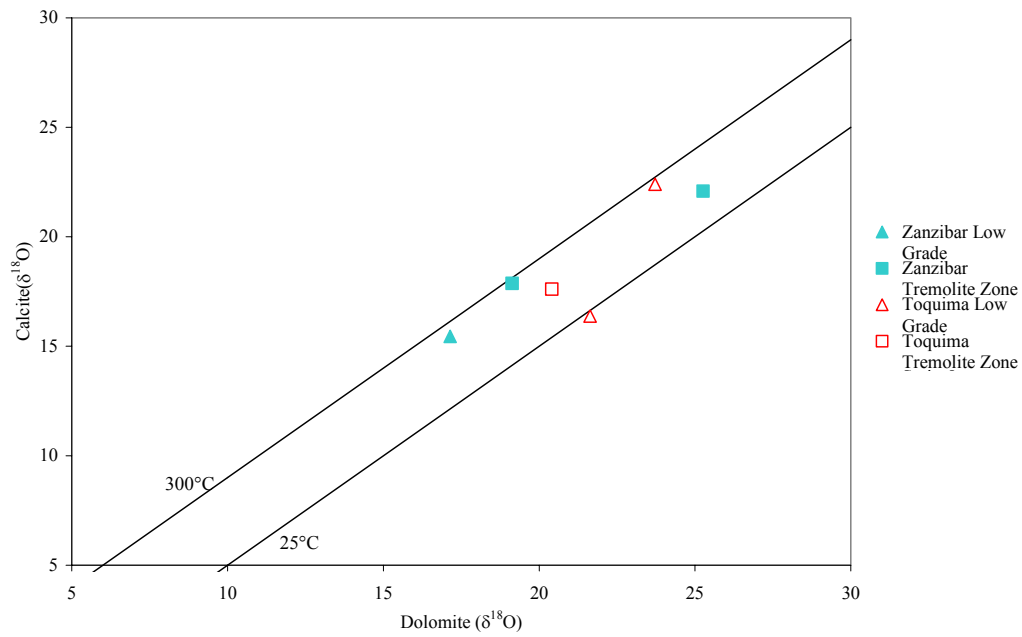


Figure A-18. Plot of $\delta^{18}\text{O}$ dolomite and calcite values for Zanzibar (blue) and Toquima (red) limestones. The lines represent fractionation ratios. These samples seem to follow the 1/1 fractionation trend. Equilibrium fractionation lines of 300°C and 25°C are from Sheppard and Schwarcz (1970).

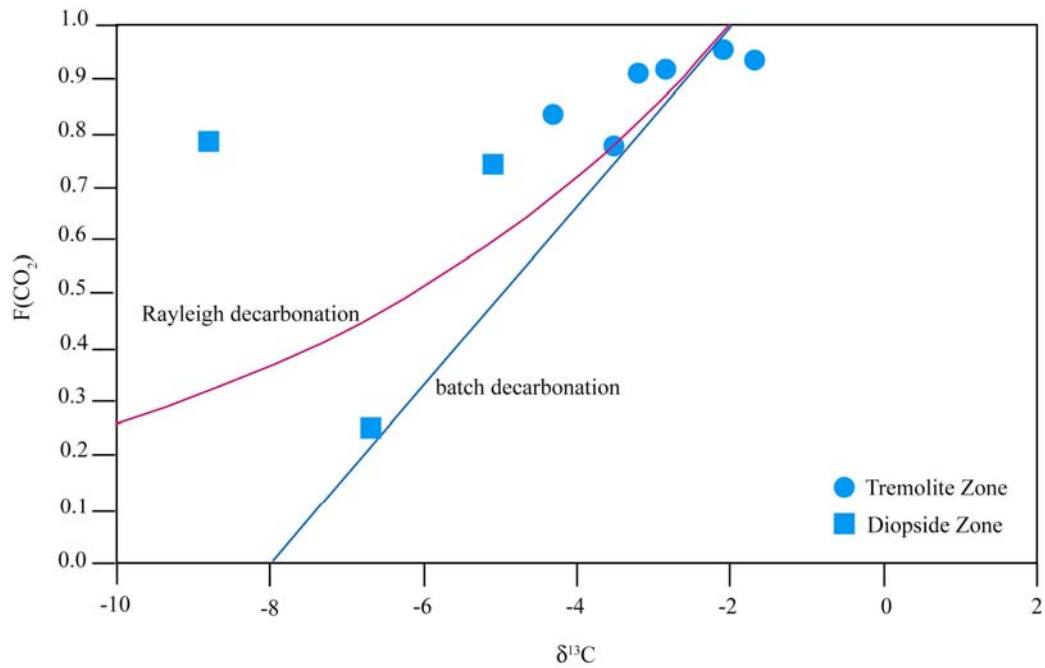


Figure A-19. Plot of $\delta^{13}\text{C}$ and $F(\text{CO}_2)$ for nine Zanzibar samples. The most of the carbon values are above the Rayleigh and batch decarbonation envelope. This indicates these values were affected by calcite exchanging with isotopically lighter carbon.

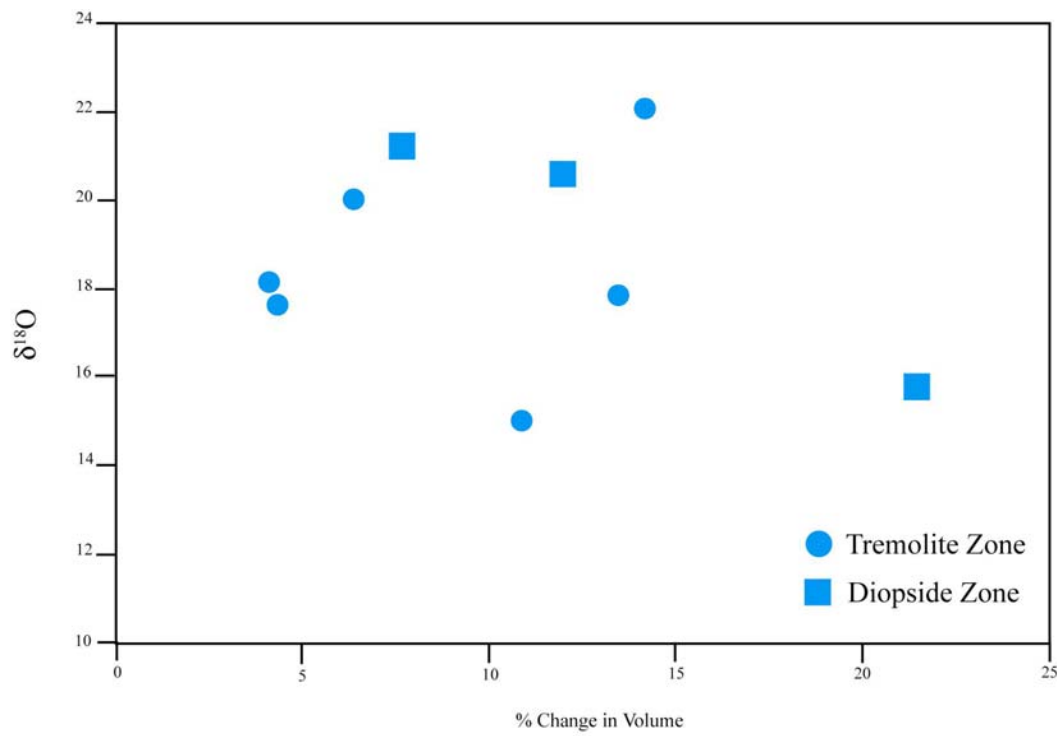


Figure A-20. Plot of calcite $\delta^{18}\text{O}$ and change in volume values for Zanzibar marbles. The different symbols indicate the metamorphic grade of the sample.

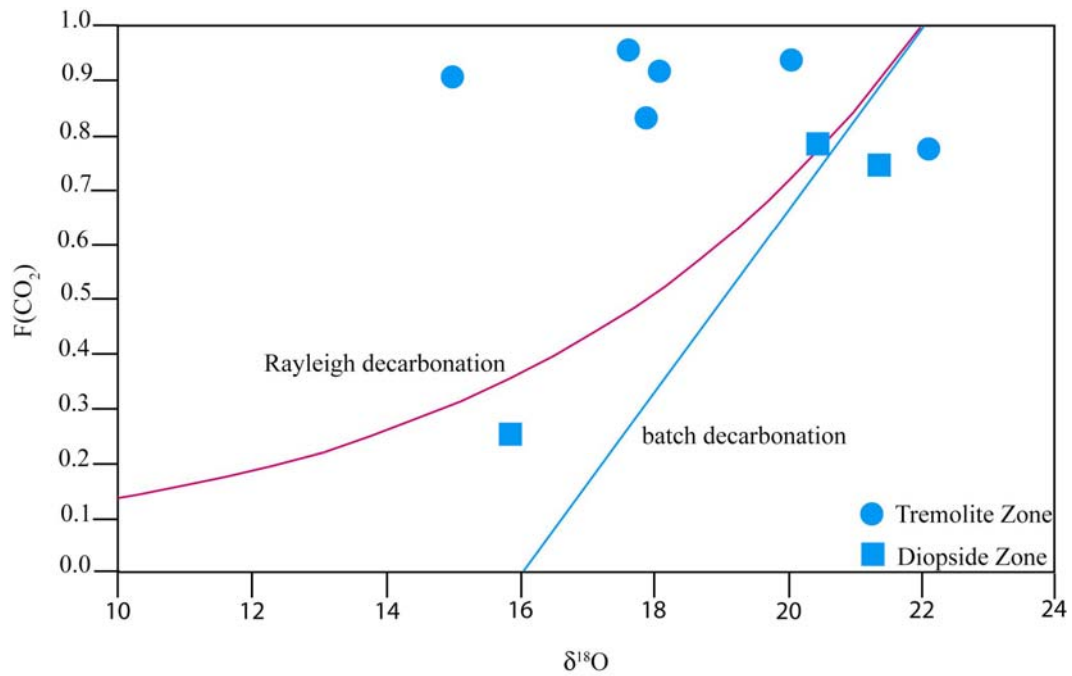


Figure A-21. Plot of $\delta^{18}\text{O}$ and $F(\text{CO}_2)$ for nine Zanzibar samples. The most of the oxygen values are above the Rayleigh and batch decarbonation envelope. This indicates these values were affected by something else besides decarbonation.

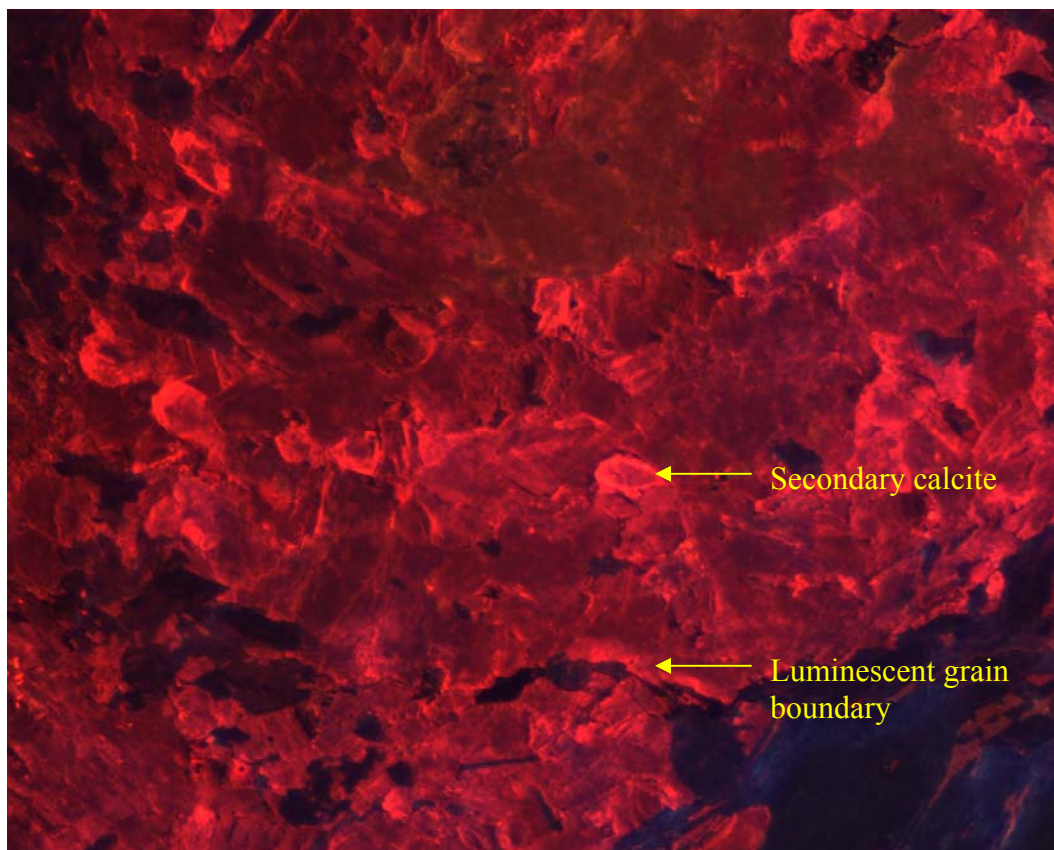


Figure A-22. CL image of a Zanzibar sample showing secondary calcite and luminescent grain boundaries.

Table B-1. Whole rock analysis. (a) for low grade marbles

Sample:	29	31	38	39	40b	50	69	SC-07	SC-08
SiO ₂	14.38	1.17	13.28	20.55	60.55	7.74	88.85	6.11	10.85
TiO ₂	0.01	0.01	0.04	0.06	0.02	0.02	0.03	0.01	0.02
Al ₂ O ₃	0.00	0.00	0.81	1.79	0.43	0.15	0.70	0.00	0.17
Fe ₂ O ₃	0.14	0.05	0.23	0.42	0.20	0.17	0.30	0.03	0.52
MnO	0.03	0.00	0.01	0.01	0.00	0.01	0.00	0.00	0.02
MgO	12.89	21.18	0.00	1.09	0.57	0.37	0.71	20.76	1.65
CaO	28.45	30.13	39.54	31.64	19.27	44.75	4.28	27.02	39.77
NaO	0.14	0.24	0.01	0.03	0.10	0.05	0.29	0.26	0.01
K ₂ O	0.00	0.00	0.73	1.56	0.02	0.04	0.36	0.00	0.02
P ₂ O ₅	0.08	0.45	0.05	0.05	0.22	0.04	0.39	0.09	0.12
Total	56.12	53.23	54.68	57.20	81.39	53.33	95.92	54.28	53.15
Trace Elements (ppm)									
S	63	3	1	10	0	67	0	0	4
Cl	0	1	0	0	0	0	108	3	0
Rb	19	22	20	20	2	21	13	21	18
Ba	8	8	8	8	0	7	409	8	8
Pb	88	88	88	89	22	88	33	88	88
Sr	21	26	113	139	8	80	37	13	11
Cr	12	7	6	5	10	9	12	3	12
Ni	173	176	426	194	0	401	0	91	72
Co	8	15	6	5	0	8	0	13	6
As	73	135	162	394	4	129	0	100	94
Nb	149	51	9	44	0	34	2	50	73
Cu	3	9	17	22	5	9	0	5	5
Cd	0	7	0	3	0	0	0	6	9

Table B-1 Continued. (b) for tremolite zone marbles.

Sample:	17a	18	44b	49	53	60	62a	62b	71
SiO ₂	5.62	13.52	29.92	23.17	55.26	9.24	4.37	90.93	17.53
TiO ₂	0.01	0.09	0.02	0.01	0.06	0.02	0.03	0.01	0.02
Al ₂ O ₃	0.00	1.87	0.04	0.00	1.71	0.03	0.22	0.24	0.06
Fe ₂ O ₃	0.50	1.30	0.11	0.12	0.37	0.10	0.10	0.17	0.15
MnO	0.02	0.01	0.01	0.01	0.01	0.02	0.01	0.00	0.04
MgO	19.35	7.14	12.44	17.02	2.10	3.21	21.18	3.54	17.32
CaO	29.85	34.61	24.17	24.24	14.23	42.76	28.83	3.46	25.19
NaO	0.23	0.09	0.15	0.20	0.04	0.03	0.24	0.26	0.21
K ₂ O	0.00	0.61	0.00	0.00	0.73	0.00	0.14	0.04	0.00
P ₂ O ₅	0.03	0.09	0.14	0.68	0.06	0.06	0.14	0.07	0.07
Total	55.63	59.34	67.00	65.45	74.57	55.46	55.26	98.71	98.71
Trace Elements (ppm)									
S	2	32	9	3	0	22	3	37	0
Cl	1	0	0	0	5	0	0	0	0
Rb	19	19	14	21	15	19	20	0	17
Ba	8	8	8	7	10	7	9	583	7
Pb	88	90	88	88	89	88	88	33	88
Sr	19	52	4	3	104	130	20	9	15
Cr	3	14	0	4	0	13	9	8	0
Ni	140	120	122	104	540	994	121	0	170
Co	11	5	0	2	0	7	13	0	2
As	66	802	148	45	465	406	177	0	70
Nb	0	33	0	0	54	6	0	1	0
Cu	6	14	0	0	8	9	18	0	0
Cd	0	12	0	0	0	1	15	0	0

Table B-1. Continued. (c) for diopside zone marbles.

Sample:	8b	SC-01	SCK-03	SCK-06
SiO ₂	52.64	54.20	42.65	45.26
TiO ₂	0.26	0.23	0.38	0.42
Al ₂ O ₃	5.92	6.33	9.31	10.32
Fe ₂ O ₃	1.82	2.22	2.95	3.84
MnO	0.04	0.04	0.03	0.03
MgO	12.19	4.23	3.93	3.87
CaO	22.76	14.58	25.11	21.13
NaO	0.82	1.15	0.26	1.00
K ₂ O	1.41	1.33	3.15	2.42
P ₂ O ₅	0.46	0.16	0.24	0.23
Total	98.30	84.45	88.00	88.50
Trace Elements (ppm)				
S	0	399	178	641
Cl	0	7	70	0
Rb	84	18	100	85
Ba	479	10	2439	2030
Pb	13	94	13	13
Sr	127	99	385	417
Cr	39	47	70	67
Ni	0	500	0	0
Co	0	0	0	0
As	0	2530	7	3
Nb	4	54	2	2
Cu	13	32	29	15
Cd	0	64	0	0

Table B-2. Mineral assemblages of Zanzibar and Toquima marbles

	Quartz	Calcite	Dolomite	Tremolite	Diopside	Muscovite	Magnetite	Graphite
Low Grade								
28	x	x						x
29	x	x	x					x
31	x		x					x
35	x	x	x					
37	x	x						
38	x	x				x		x
39	x	x				x		x
40b	x	x						
50	x	x						
64	x	x						x
69	x	x						
SC04	x	x	x			x		
SC05		x	x					
SC07	x	x	x					
SC08	x	x	x					
SC13	x	x						
Tremolite Zone								
7b	x	x		x				
12a	x	x	x	x				x
17a		x	x	x				x
18		x		x		x	x	x
19	x			x				x
22b		x		x				
22a		x		x				x
23a		x		x		x	x	x
23b		x		x				x
26	x			x				

Table B-2. Continued

	Quartz	Calcite	Dolomite	Tremolite	Diopside	Muscovite	Magnetite	Graphite
Tremolite Zone								
34	x			x				
42		x		x				
44a		x		x				
44b		x		x				x
47		x		x				x
49		x	x	x				x
51		x		x				
52	x			x				
53	x	x		x		x		x
54	x	x		x				x
55	x	x		x				x
56	x			x				
58	x	x		x				x
59		x		x				x
60	x	x		x				x
62a	x	x		x				x
68	x	x		x				
69	x	x		x				
71		x	x	x				x
72	x	x	x	x		x		
SC06	x	x		x				x
SC10	x	x		x				x
SCK04	x	x		x				

Table B-2. Continued

	Quartz	Calcite	Dolomite	Tremolite	Diopside	Muscovite	Magnetite	Graphite
Diopside Zone								
8b	x	x			x	x	x	
9b	x	x			x			x
SC01	x				x	x	x	
SC02	x				x	x	x	
SC03	x	x			x			
SC04	x	x			x			
SCK03	x	x			x	x	x	x
SCK06	x	x			x	x	x	x
SCK07	x	x			x	x	x	x

Table B-3. Metamorphic mass-balance

		Quartz	Calcite	Dolomite	Tremolite	Diopside	Muscovite	Magnetite	H ₂ O	CO ₂	Volume (cm ³)
Tremolite Zone											
17a	Before Metamorphism	56.1	52.3	883.2	0.0	0.0	0.0	0.0	0.0	117.1	351.7
	After Metamorphism	0.0	87.4	775.6	94.8	0.0	0.0	0.0	0.4	112.0	336.5
18	Before Metamorphism	124.0	440.0	325.9	0.0	0.0	24.6	0.6	0.1	135.8	337.3
	After Metamorphism	0.0	517.5	89.2	209.6	0.0	24.6	0.6	1.4	123.4	300.6
49	Before Metamorphism	231.5	10.0	776.5	0.0	0.0	0.0	0.0	0.0	95.0	365.4
	After Metamorphism	0.0	154.5	333.3	391.1	0.0	0.0	0.0	0.4	73.7	313.8
53	Before Metamorphism	541.7	201.7	95.7	0.0	0.0	23.1	0.0	0.0	55.8	327.3
	After Metamorphism	491.7	232.9	0.0	84.4	0.0	23.1	0.0	0.5	51.3	313.8
60	Before Metamorphism	83.3	705.1	135.4	0.0	0.0	0.0	0.0	0.0	171.3	339.6
	After Metamorphism	16.0	730.7	0.0	129.0	0.0	0.0	0.0	0.1	160.8	318.0
62b	Before Metamorphism	908.5	0.0	161.5	0.0	0.0	0.0	0.0	0.0	19.3	403.5
	After Metamorphism	815.5	0.0	0.0	157.2	0.0	0.0	0.0	0.2	0.0	362.7
71	Before Metamorphism	175.1	19.6	790.5	0.0	0.0	0.0	0.0	0.0	98.8	352.4
	After Metamorphism	0.0	128.9	455.1	295.8	0.0	0.0	0.0	0.3	82.8	304.8
Diopside Zone											
8b	Before Metamorphism	525.9	103.5	556.2	0.0	0.0	75.4	8.8	0.0	89.3	463.9
	After Metamorphism	162.9	103.5	0.0	0.0	848.2	75.4	8.8	0.0	22.8	364.9
SCK03	Before Metamorphism	426.1	350.4	179.0	0.0	0.0	122.4	14.3	0.0	98.5	399.4
	After Metamorphism	288.6	333.8	0.0	0.0	319.9	122.4	14.3	0.0	77.1	352.0
SCK06	Before Metamorphism	452.2	280.8	176.5	0.0	0.0	119.3	18.6	0.0	82.9	363.2
	After Metamorphism	311.0	259.1	0.0	0.0	330.0	119.3	18.6	0.0	61.8	335.9

Table B-4. Calcite isotopic values

	O^{18} (SMOW)	C^{13} (PDB)
Low Grade		
29	16.4	-2.1
31	21.4	-0.8
38	18.6	-1.8
39	11.0	-2.4
40b	12.3	-1.1
69	19.6	-6.5
SC07	22.4	-1.1
SC08	15.5	-4.6
Tremolite Zone		
42	18.6	-8.1
18	15.0	-3.2
17a	17.6	-2.1
41	18.9	-7.9
44b	17.7	-4.4
49	22.1	-3.5
53	18.1	-2.9
58	19.8	-5.8
60	20.0	-1.7
62a	24.5	-1.2
71	17.9	-4.3
Diopside Zone		
8b	15.7	-6.7
12a	19.4	-2.2
SCK03	20.5	-9.0
SCK06	21.2	-5.2

Table B-5. Dolomite isotope values

	O^{18} (SMOW)	C^{13} (PDB)
Low Grade		
29	21.6	-0.7
31	21.4	-0.8
SC07	23.7	-0.6
SC08	17.1	-3.3
Tremolite Zone		
17a	20.4	-1.2
49	25.3	-2.8
71	19.1	-3.4

Vita

Kelly Ross Plummer was born in Charlotte, North Carolina on December 30, 1979. He was raised in Concord, North Carolina and attended grade school at Harrisburg Elementary and J. N. Fries Middle School. He graduated from Central Cabarrus High School in 1998. From there, he attended the University of North Carolina at Charlotte where he received a B. S. in Geology in 2002. In 2006 he received a M. S. in Geology from the University of Tennessee at Knoxville. Kelly is currently living in Charlotte, North Carolina seeking employment in geology or a related field.